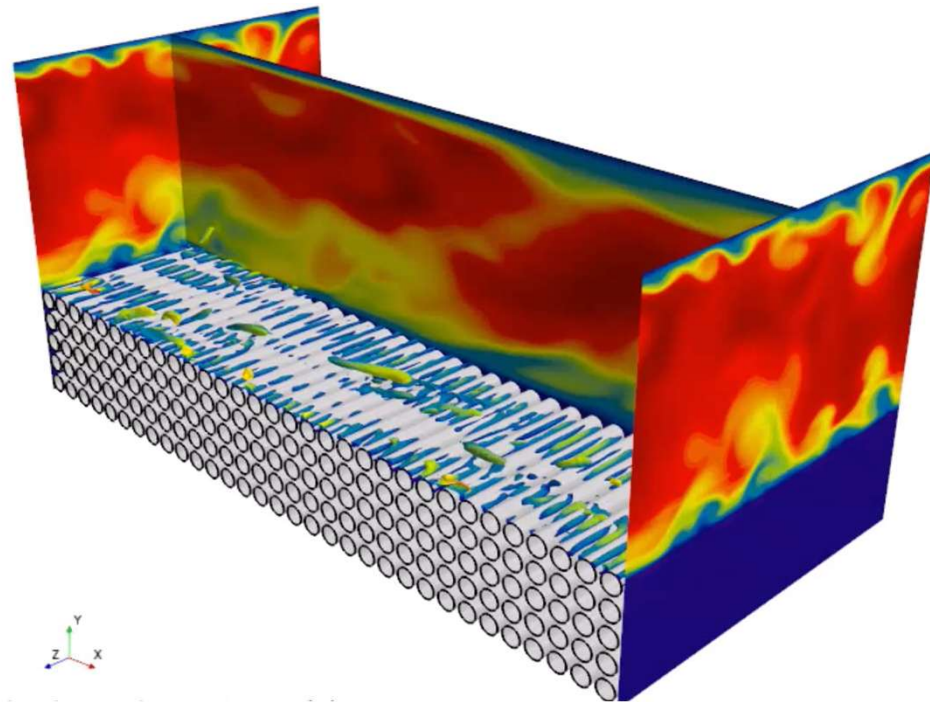
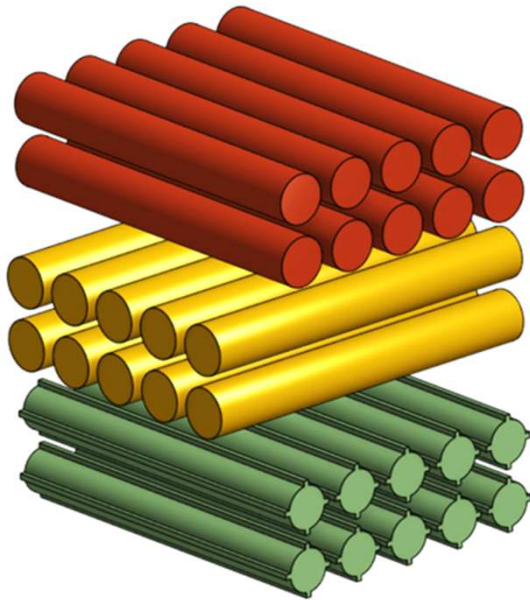
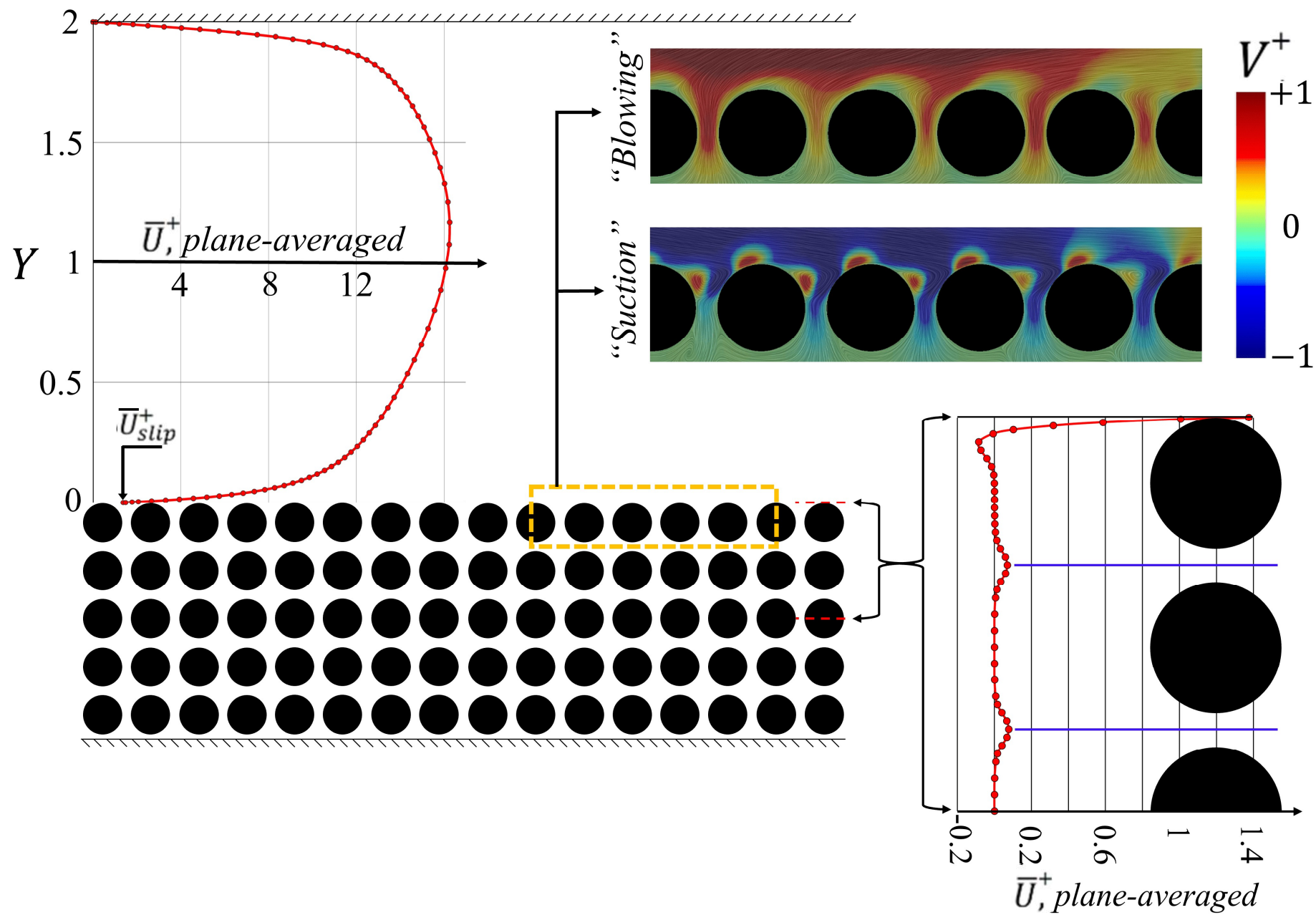


# Turbulent flow over a porous wall

Essam Nabil Ahmed & Alessandro Bottaro

DICCA, Università di Genova, Italy

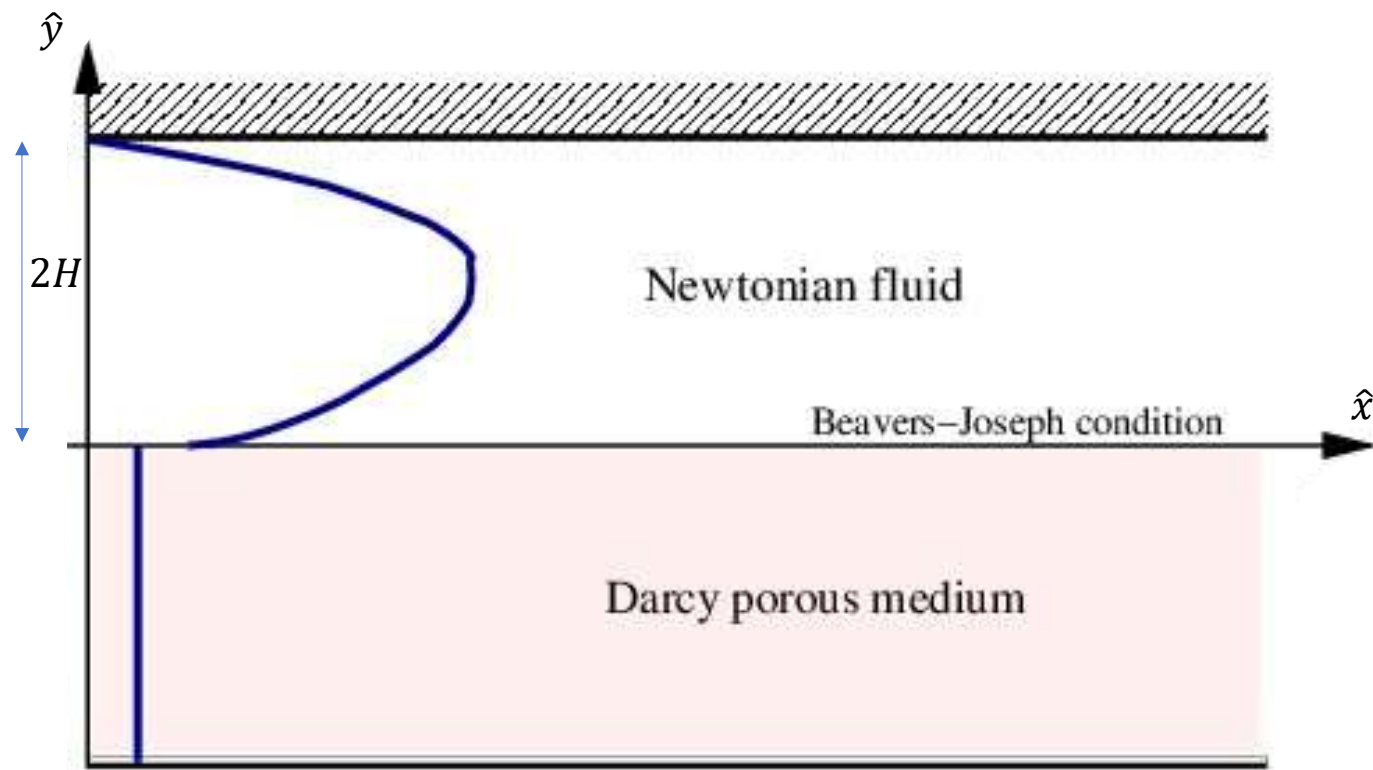




Can we model the presence of the permeable substrate without solving for the flow through the porous medium? Can we find *effective* boundary conditions at a virtual wall which

(1) can be derived rigorously and

(2) actually work (and not only in the laminar case)?!



**Accounting for transpiration at the fictitious wall is essential**

# Generalized slip condition over rough surfaces

Giuseppe A. Zampogna<sup>1</sup>, Jacques Magnaudet<sup>1</sup> and Alessandro Bottaro<sup>2,†</sup>

<sup>1</sup>Institut de Mécanique des Fluides de Toulouse (IMFT), Université de Toulouse, CNRS, INPT, UPS, 31400 Toulouse, France

<sup>2</sup>Dipartimento di Ingegneria Civile, Chimica e Ambientale, Università di Genova, Via Montallegro 1, 16145 Genova, Italy

(Received 22 December 2017; revised 25 September 2018; accepted 25 September 2018)

$$u_i = \epsilon \mathcal{L}_{ilk} \left( \frac{\partial u_l}{\partial x_k} + \frac{\partial u_k}{\partial x_l} \right) \Big|_{\text{ES}}$$

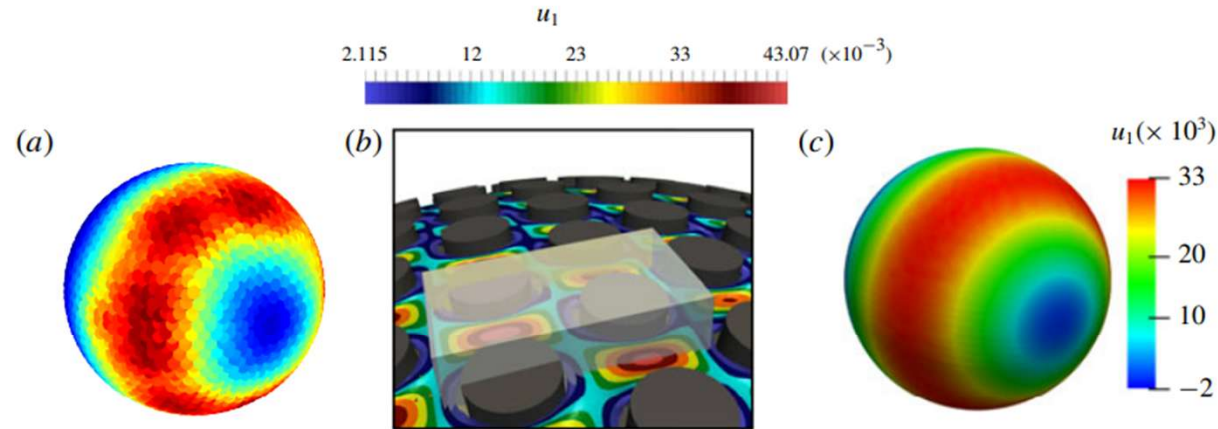


FIGURE 9. (Colour online) Comparison of the streamwise velocity component,  $u_1$ , on the sphere, computed with the macroscopic model (2.28) (c), and extracted from the reference DNS (a). The procedure used to pass from one approach to the other is detailed in the text. (b) The microscopic cell,  $V$ , (in grey), with the microscopic distribution of the  $u_1$  iso-contours on a surface located slightly above  $R = 1$ .

**Can we do more?**

# Can we do more?

- Extend to **higher order** in  $\epsilon$

# Can we do more?

- Extend to **higher order** in  $\epsilon$
- Account for **near-wall inertia** and make the simplified procedure (with *effective* boundary conditions at the wall) work for the case of turbulent flow



# Can we do more?

- Extend to **higher order** in  $\epsilon$
- Account for **near-wall inertia** and make the simplified procedure (with *effective* boundary conditions at the wall) work for the case of turbulent flow
- Find a relation that permits to determine  $\Delta U^+$  (roughness function) and the slip velocity  $\overline{U}_{slip}^+$  directly from macroscopic upscaling coefficients

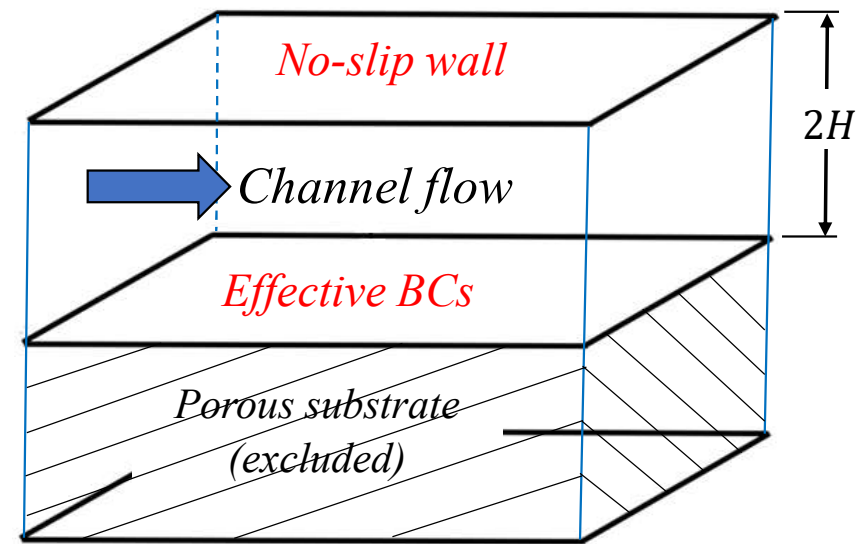
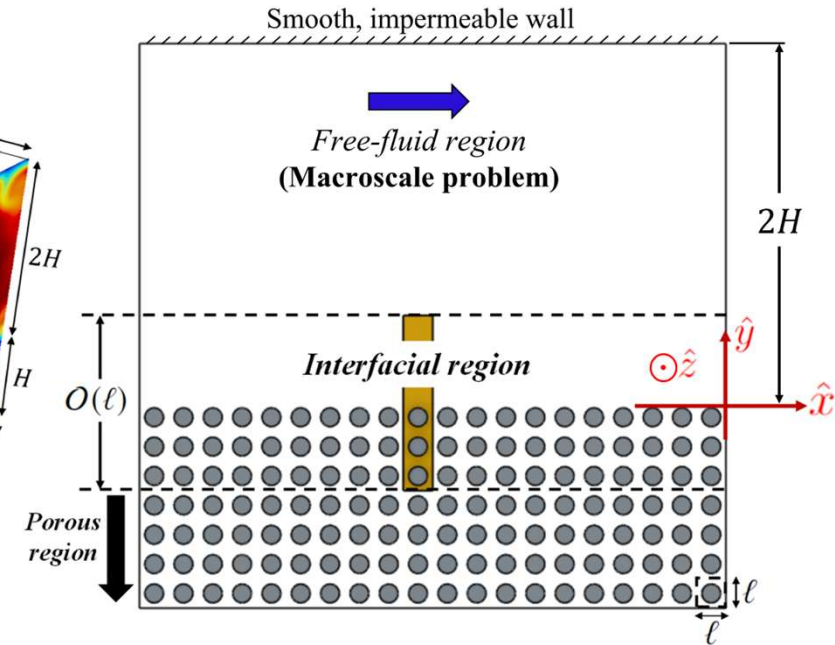
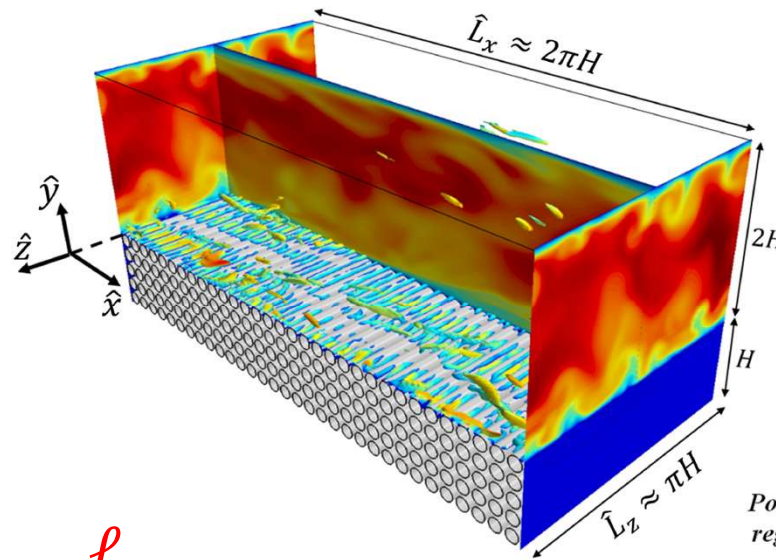
Rapidly-varying properties  
(related to surface heterogeneity)

Homogenization  
framework

Upscaled, homogeneous properties  
(for *effective* boundary conditions)

Navier-slip coefficients,  
intrinsic permeability,  
interfacial permeability,  
etc.

$$\epsilon = \frac{\ell}{H} \ll 1$$



## Macroscopic *effective* boundary conditions

$$U \Big|_{Y=0^+} = \underbrace{\epsilon \lambda_x S_{12} \Big|_{Y=0^+}}_{\text{Navier-slip condition}} + \underbrace{\epsilon^2 \mathcal{K}_{xy}^{itf} \frac{\partial S_{22}}{\partial X} \Big|_{Y=0^+}}_{\text{Second-order correction}} + \mathcal{O}(\epsilon^3)$$

$$S_{12} = \frac{\partial U}{\partial Y} + \frac{\partial V}{\partial X},$$

$$S_{22} = -Re P + 2 \frac{\partial V}{\partial Y},$$

$$S_{32} = \frac{\partial W}{\partial Y} + \frac{\partial V}{\partial Z}.$$

$$V \Big|_{Y=0^+} = \underbrace{-\epsilon^2 \mathcal{K}_{xy}^{itf} \frac{\partial S_{12}}{\partial X} \Big|_{Y=0^+} - \epsilon^2 \mathcal{K}_{zy}^{itf} \frac{\partial S_{32}}{\partial Z} \Big|_{Y=0^+}}_{\text{Second-order, effect of interface permeabilities}} + \underbrace{\epsilon^2 \mathcal{K}_{yy} \frac{\partial S_{22}}{\partial Y} \Big|_{Y=0^+}}_{\text{Second-order, effect of medium permeability}} + \mathcal{O}(\epsilon^3)$$

$$W \Big|_{Y=0^+} = \underbrace{\epsilon \lambda_z S_{32} \Big|_{Y=0^+}}_{\text{Navier-slip condition}} + \underbrace{\epsilon^2 \mathcal{K}_{zy}^{itf} \frac{\partial S_{22}}{\partial Z} \Big|_{Y=0^+}}_{\text{Second-order correction}} + \mathcal{O}(\epsilon^3)$$

$\lambda_{x,z}$ : Navier-slip coefficients

$\mathcal{K}_{xy,zy}^{itf}$ : Interface permeability coefficients

$\mathcal{K}_{yy}$ : medium permeability

# Near-wall advection modeling

- An **Oseen-like linearization** was proposed to include the effects of near-interface advection in the homogenization scheme (Bottaro A., *J. Fluid Mech.* (2019), vol. 877, P1)
- We define a spatially invariant velocity  $\hat{\mathbf{u}}_{\phi,j} = (\hat{\mathbf{u}}_{\phi}, \mathbf{0}, \mathbf{0})$ , representative of the near-wall velocity level.
- Governing equations of the microscale problem: 
$$\frac{\partial \hat{u}_i}{\partial \hat{x}_i} = 0, \quad \rho \hat{u}_{\phi,j} \frac{\partial \hat{u}_i}{\partial \hat{x}_j} = -\frac{\partial \hat{p}}{\partial \hat{x}_i} + \mu \frac{\partial^2 \hat{u}_i}{\partial \hat{x}_j^2}$$
- The microscopic Reynolds number, defined as  $Re_{\phi} = \frac{\rho \hat{\mathbf{u}}_{\phi} \ell}{\mu} = \epsilon Re_{\tau} U_{\phi}^{+}$ , is assumed to be of order 1.

## The closure problems

$$\left\{ \begin{array}{l} \partial_i u_{i1}^{\dagger} = 0, \\ -\partial_i p_1^{\dagger} + \partial_k^2 u_{i1}^{\dagger} = Re_{\phi} \partial_1 u_{i1}^{\dagger}, \\ u_{i1}^{\dagger} = 0 \quad \text{at } \mathcal{I}_{\beta\sigma}, \\ -p_1^{\dagger} \delta_{i2} + \partial_2 u_{i1}^{\dagger} + \partial_i u_{21}^{\dagger} = \delta_{i1} \quad \text{at } y = y_{\infty}. \end{array} \right.$$

$$\lambda_x = \frac{1}{\mathcal{A}} \int_{S_0} u_{11}^{\dagger} dA$$

$$\mathcal{K}_{xy}^{itf} = \frac{1}{\mathcal{A}} \int_{\mathcal{V}_0} u_{11}^{\dagger} dV$$

$$\left\{ \begin{array}{l} \partial_i u_{i3}^{\dagger} = 0, \\ -\partial_i p_3^{\dagger} + \partial_k^2 u_{i3}^{\dagger} = Re_{\phi} \partial_1 u_{i3}^{\dagger}, \\ u_{i3}^{\dagger} = 0 \quad \text{at } \mathcal{I}_{\beta\sigma}, \\ -p_3^{\dagger} \delta_{i2} + \partial_2 u_{i3}^{\dagger} + \partial_i u_{23}^{\dagger} = \delta_{i3} \quad \text{at } y = y_{\infty}. \end{array} \right.$$

$$\lambda_z = \frac{1}{\mathcal{A}} \int_{S_0} u_{33}^{\dagger} dA$$

$$\mathcal{K}_{zy}^{itf} = \frac{1}{\mathcal{A}} \int_{\mathcal{V}_0} u_{33}^{\dagger} dV$$

$$U\Big|_{Y=0^+} = \epsilon \lambda_x \frac{\partial U}{\partial Y}\Big|_{Y=0^+} - \epsilon^2 \operatorname{Re} \mathcal{K}_{xy}^{itf} \frac{\partial P}{\partial X}\Big|_{Y=0^-} + \mathcal{O}(\epsilon^3)$$

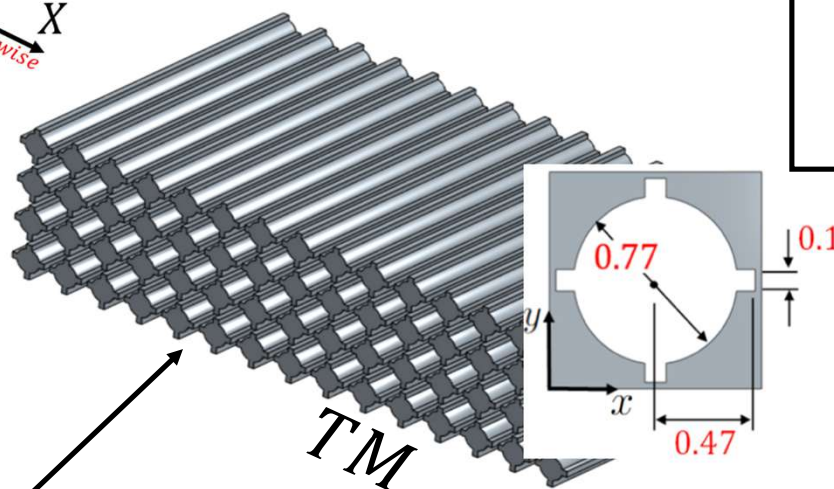
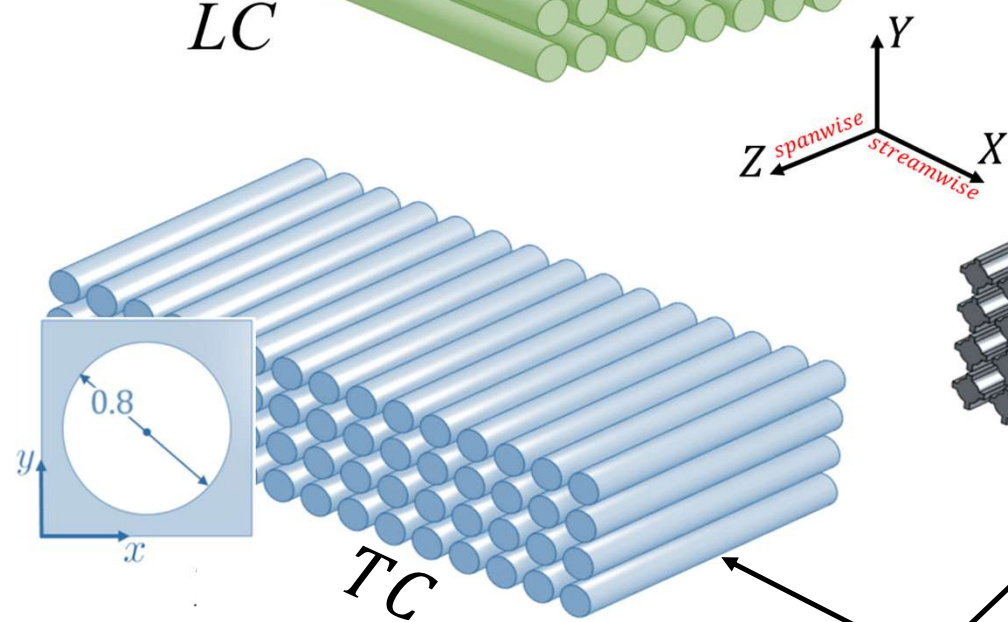
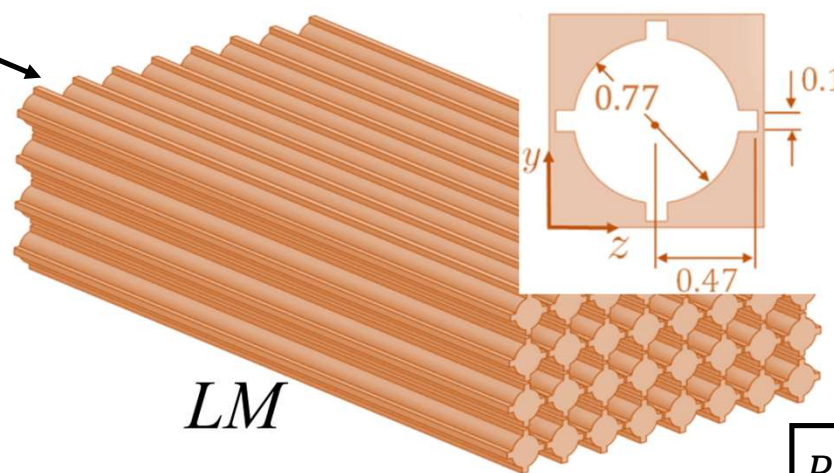
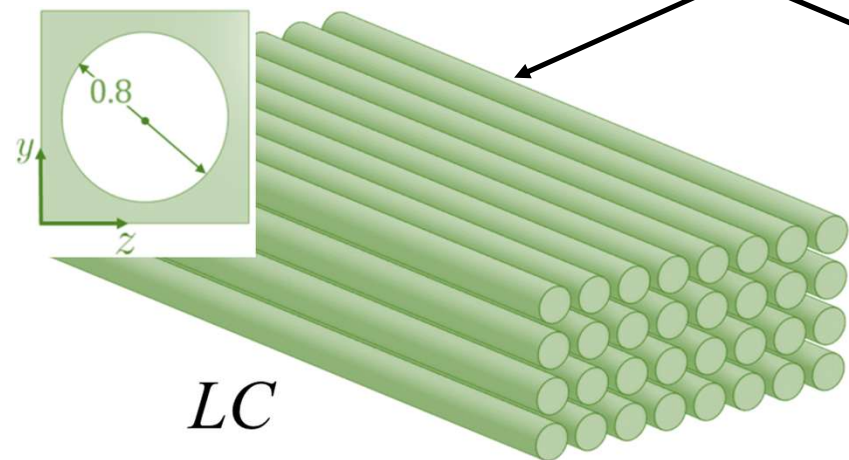
$$V\Big|_{Y=0^+} = -\epsilon \frac{\mathcal{K}_{xy}^{itf}}{\lambda_x} \frac{\partial U}{\partial X}\Big|_{Y=0^+} - \epsilon \frac{\mathcal{K}_{zy}^{itf}}{\lambda_z} \frac{\partial W}{\partial Z}\Big|_{Y=0^+} - \epsilon^2 \operatorname{Re} \mathcal{K}_{yy} \frac{\partial P}{\partial Y}\Big|_{Y=0^-} + \mathcal{O}(\epsilon^3)$$

$$W\Big|_{Y=0^+} = \epsilon \lambda_z \frac{\partial W}{\partial Y}\Big|_{Y=0^+} - \epsilon^2 \operatorname{Re} \mathcal{K}_{zy}^{itf} \frac{\partial P}{\partial Z}\Big|_{Y=0^-} + \mathcal{O}(\epsilon^3)$$

Extended Beavers-Joseph-Saffman conditions with NO empirical coefficients

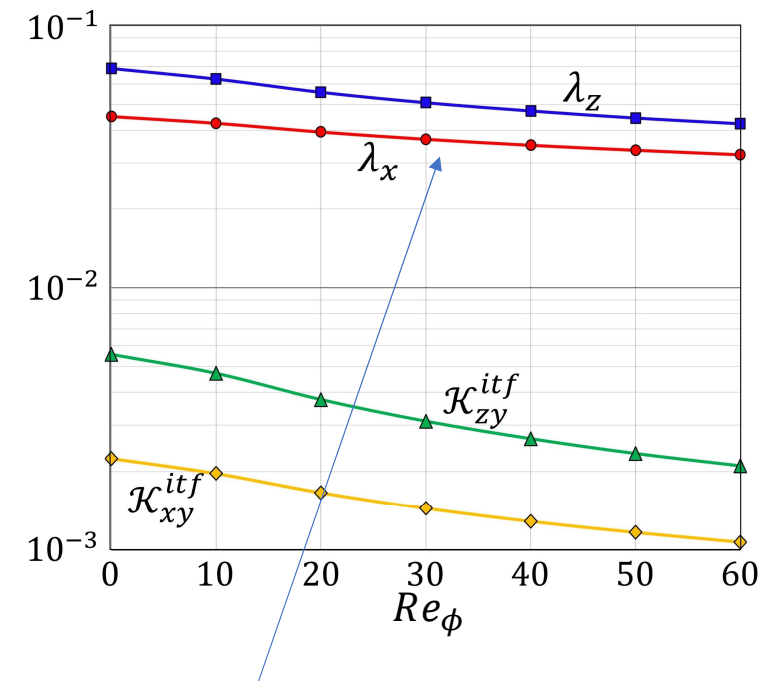
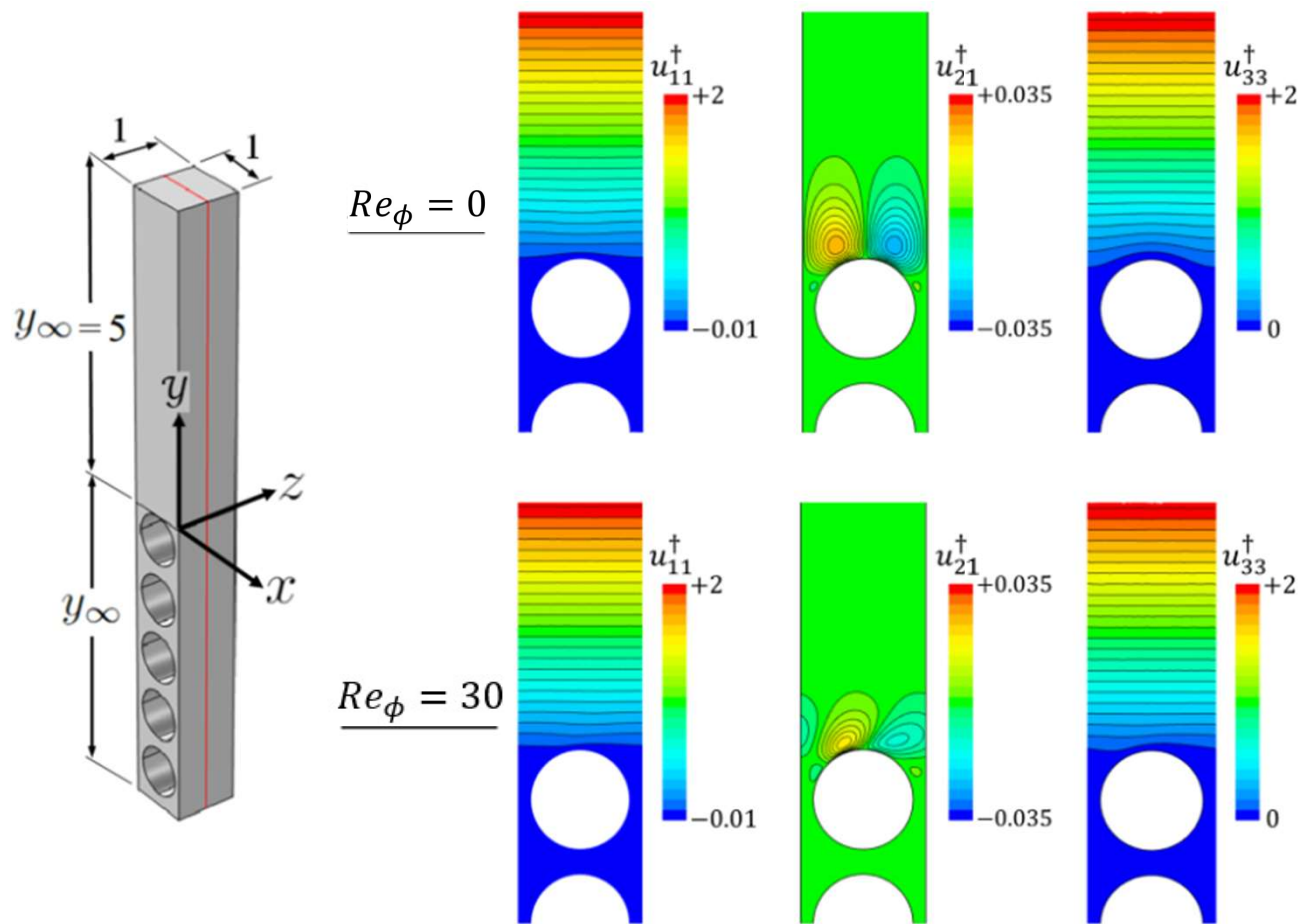


Possible drag reduction 😊

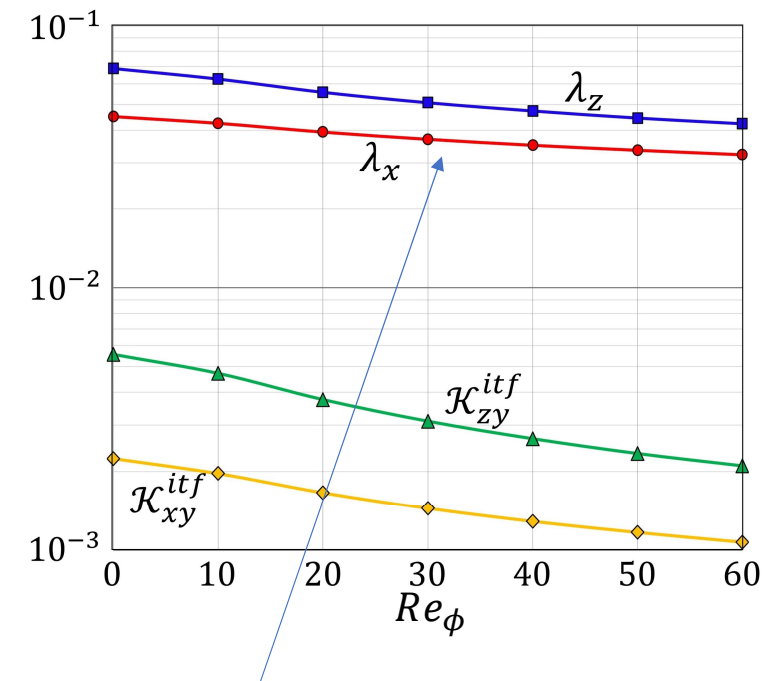
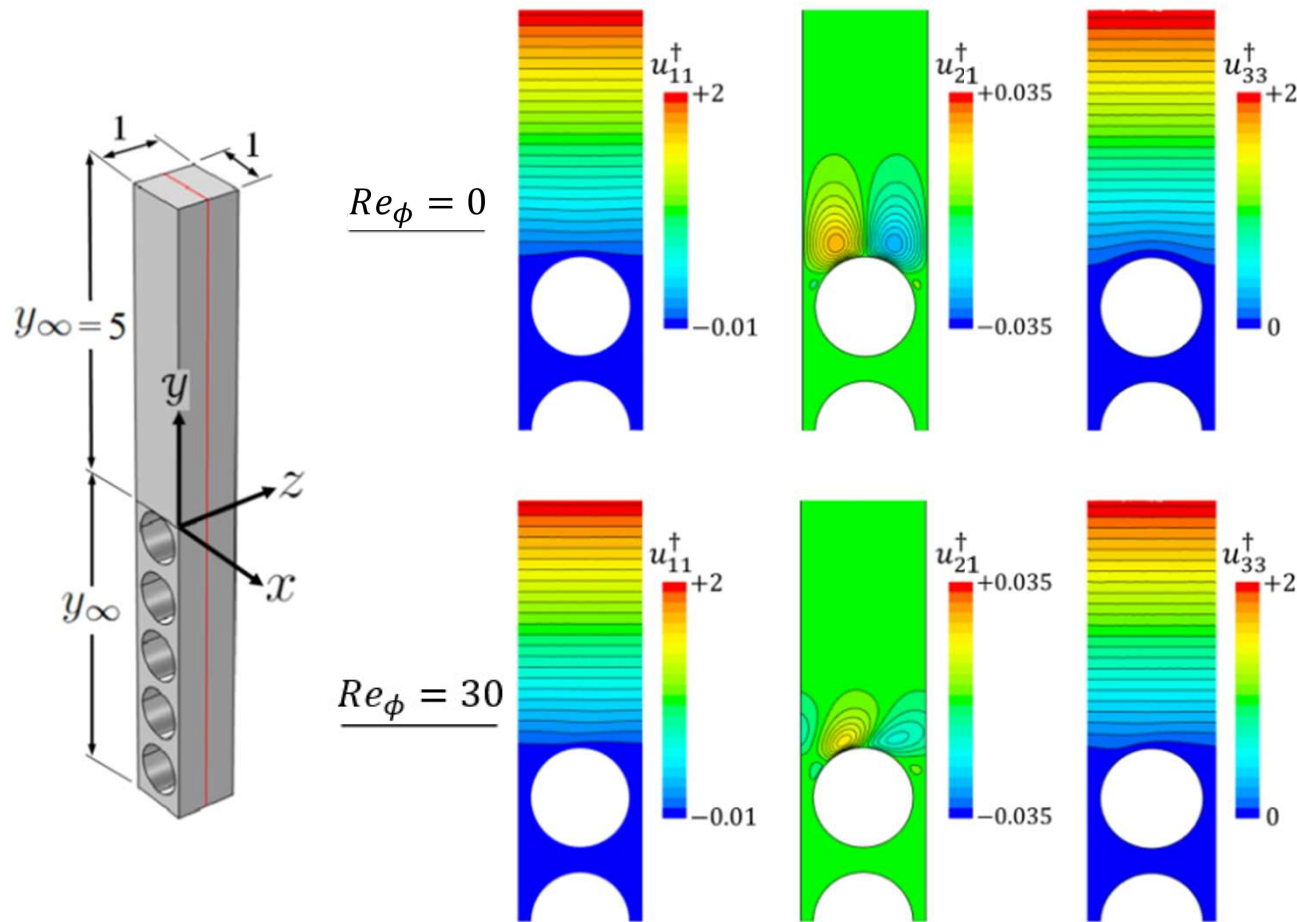


Drag increase 😞

Porosity = 0.5 for all  
 $\epsilon = 0.05 \rightarrow 0.2$   
 $Re_\tau \approx 190$



Two different virtual origins for longitudinal and transverse flow, i.e. for mean flow and for turbulence



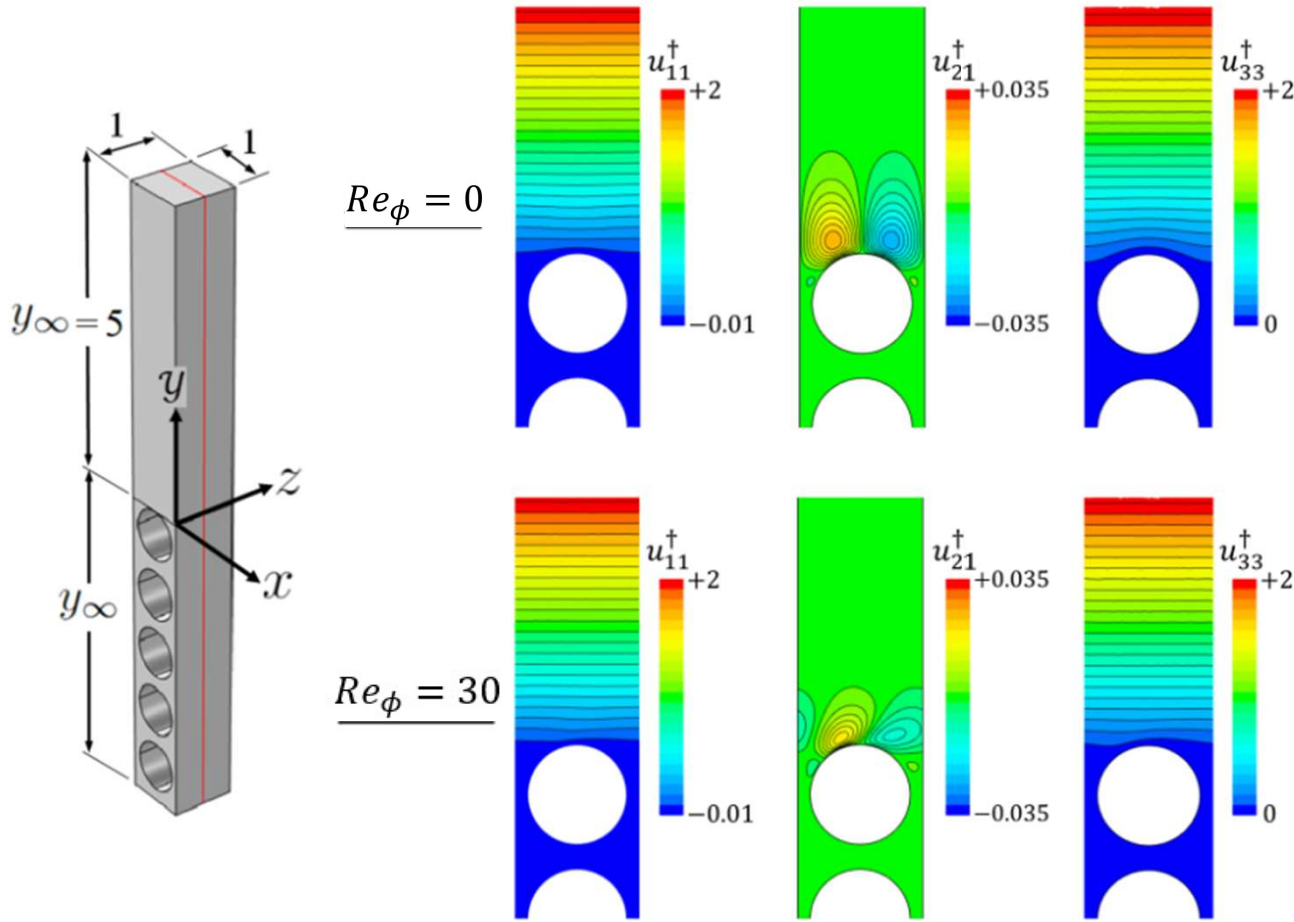
Two different virtual origins for longitudinal and transverse flow, i.e. for mean flow and for turbulence

$$\text{Assume } \hat{u}_\phi = \hat{u}_{slip} \rightarrow Re_\phi = \epsilon Re_\tau \bar{U}_{slip}^+$$

$$\text{First-order: } \bar{U}_{slip}^+ \approx \lambda_x^+ \left. \frac{\partial \bar{U}^+}{\partial Y^+} \right|_{Y=0} \approx \lambda_x^+ = \frac{\rho u_\tau \times \ell \lambda_x}{\mu} = \epsilon Re_\tau \lambda_x$$

$$\therefore Re_\phi \approx \epsilon^2 Re_\tau^2 \lambda_x$$

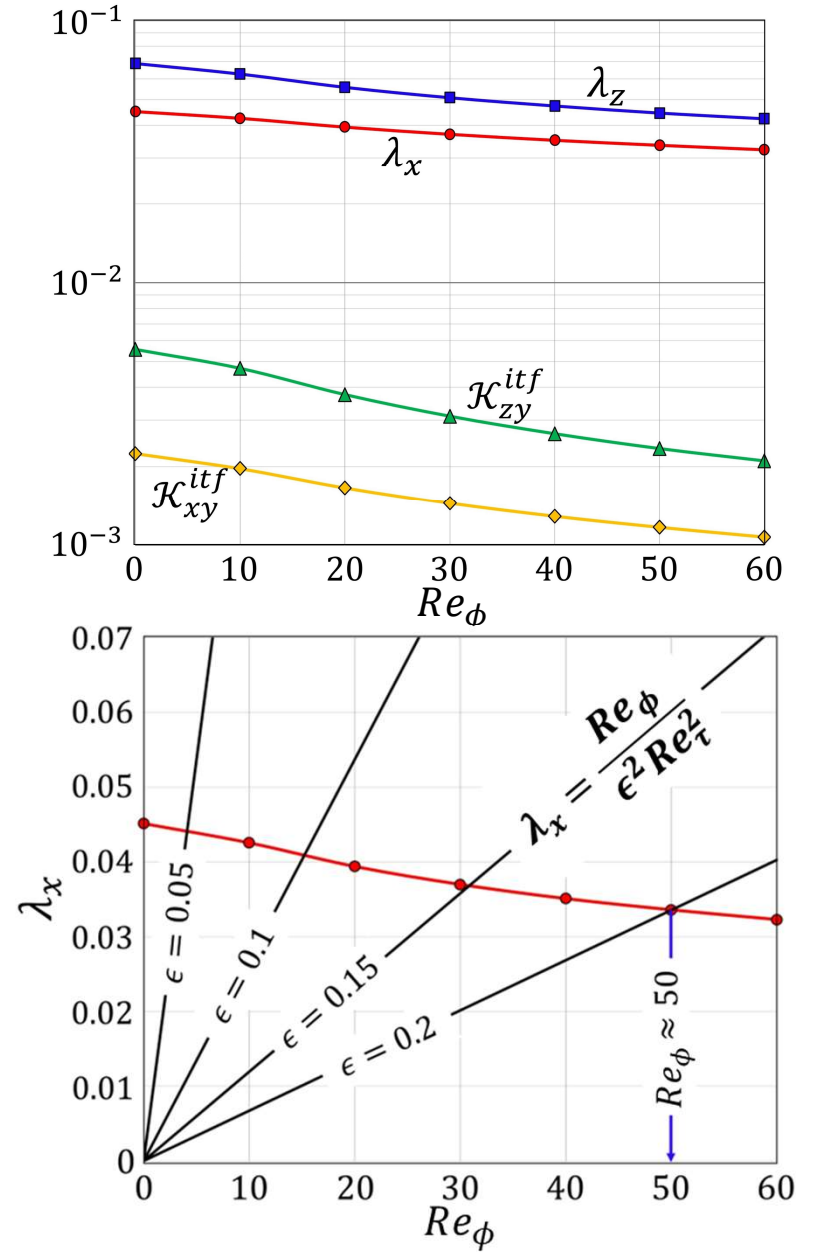




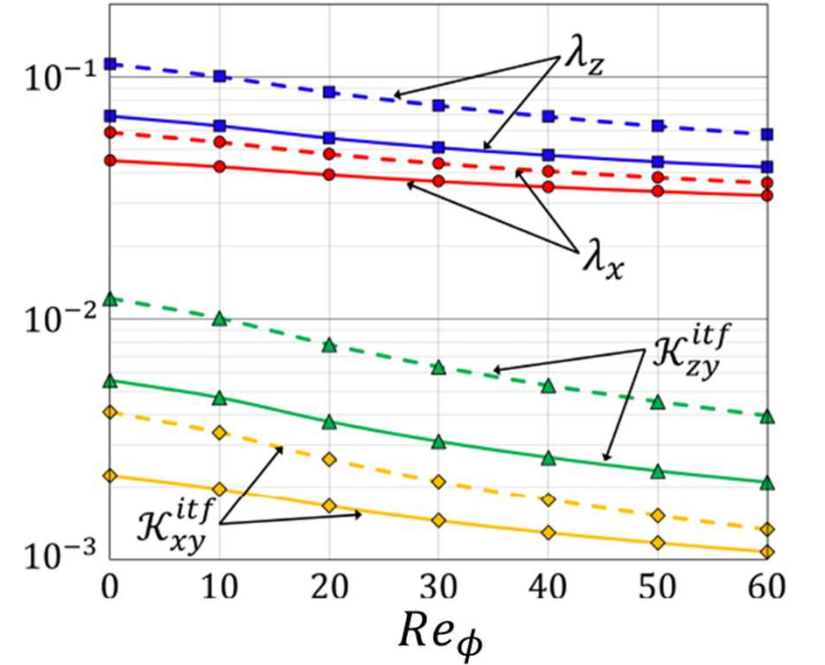
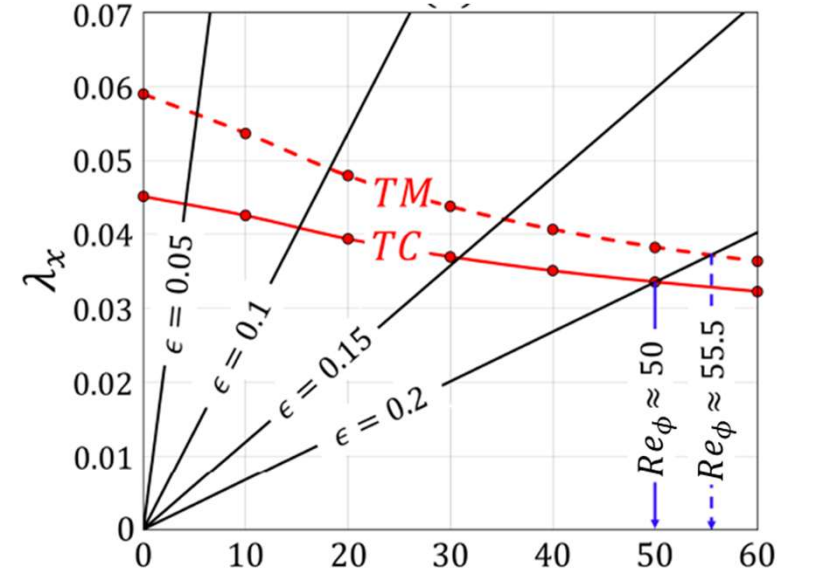
Assume  $\hat{u}_\phi = \hat{u}_{slip} \rightarrow Re_\phi = \epsilon Re_\tau \bar{U}_{slip}^+$

**First-order:**  $\bar{U}_{slip}^+ \approx \lambda_x^+ \left. \frac{\partial U^+}{\partial Y^+} \right|_{Y=0} \approx \lambda_x^+ = \frac{\rho u_\tau \times \ell \lambda_x}{\mu} = \epsilon Re_\tau \lambda_x$

$\therefore Re_\phi \approx \epsilon^2 Re_\tau^2 \lambda_x$



Substrate	$Re_\phi$ (intersection)	Dimensionless macroscopic coefficients				
		$\lambda_x$	$\lambda_z$	$\mathcal{K}_{xy}^{itf}$	$\mathcal{K}_{zy}^{itf}$	$\mathcal{K}_{yy}$
$TC_5$	4.1	0.0440	0.0663	0.0021	0.0052	0.0018
$TC_{10}$	15.2	0.0409	0.0591	0.0018	0.0042	0.0018
$TC_{15}$	30.9	0.0368	0.0506	0.0014	0.0031	0.0018
$TC_{20}$	50.0	0.0336	0.0445	0.0012	0.0023	0.0018
$LC$	Any	0.0688	0.0451	0.0056	0.0022	0.0018
$TM_5$	5.3	0.0562	0.1062	0.0037	0.0110	0.00012
$TM_{10}$	18.2	0.0489	0.0888	0.0028	0.0082	0.00012
$TM_{15}$	35.3	0.0421	0.0721	0.0019	0.0058	0.00012
$TM_{20}$	55.5	0.0372	0.0599	0.0014	0.0042	0.00012
$LM$	Any	0.1130	0.0590	0.0121	0.0041	0.00012



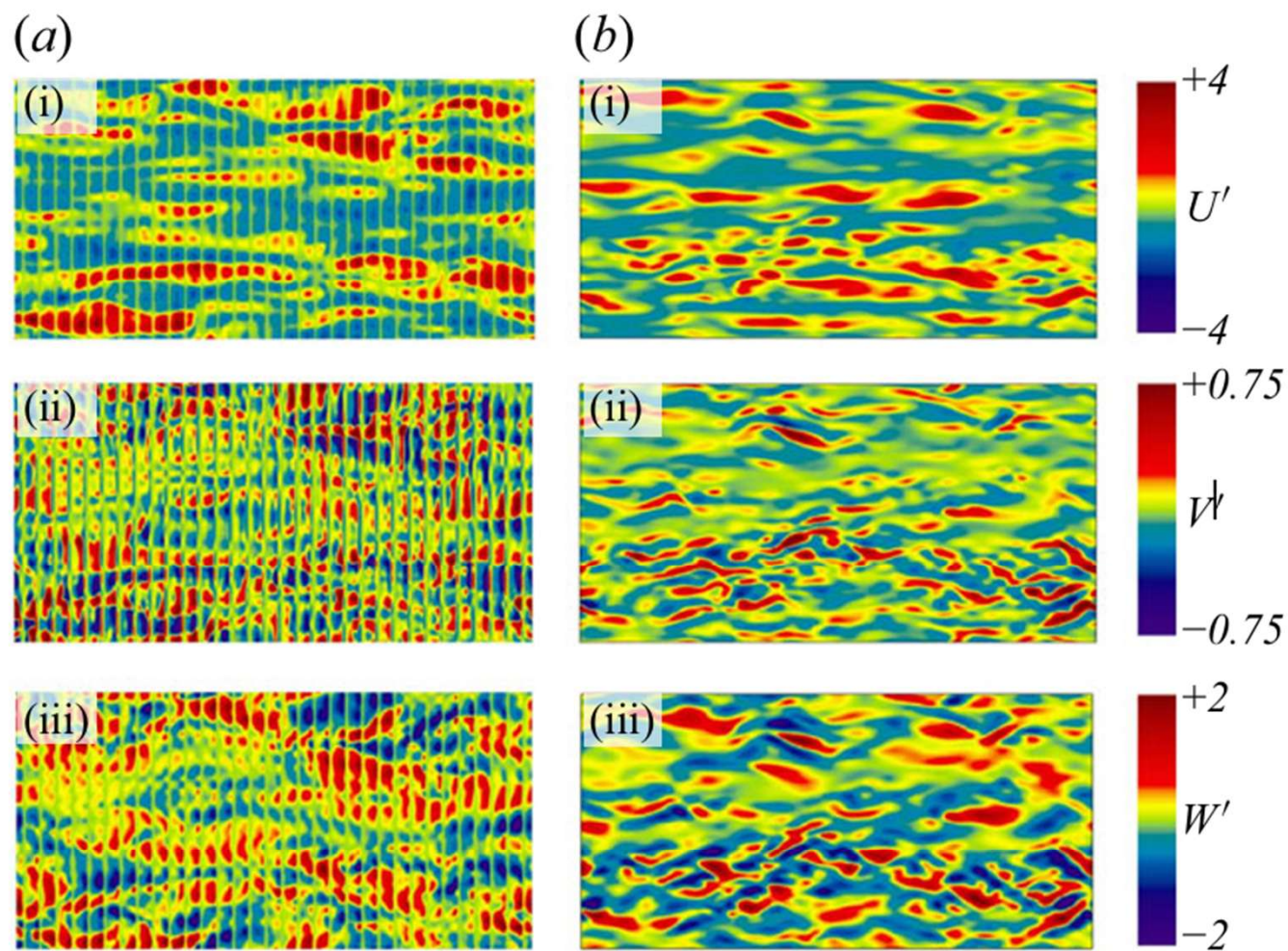


Figure 8. From (i) to (iii), instantaneous distributions of  $U'$ ,  $V'$  and  $W'$  at the porous-free-fluid interface ( $Y = 0$ ) for case  $TC_{20}$ . The fully resolved results (a) are compared with the homogenized ones (b).

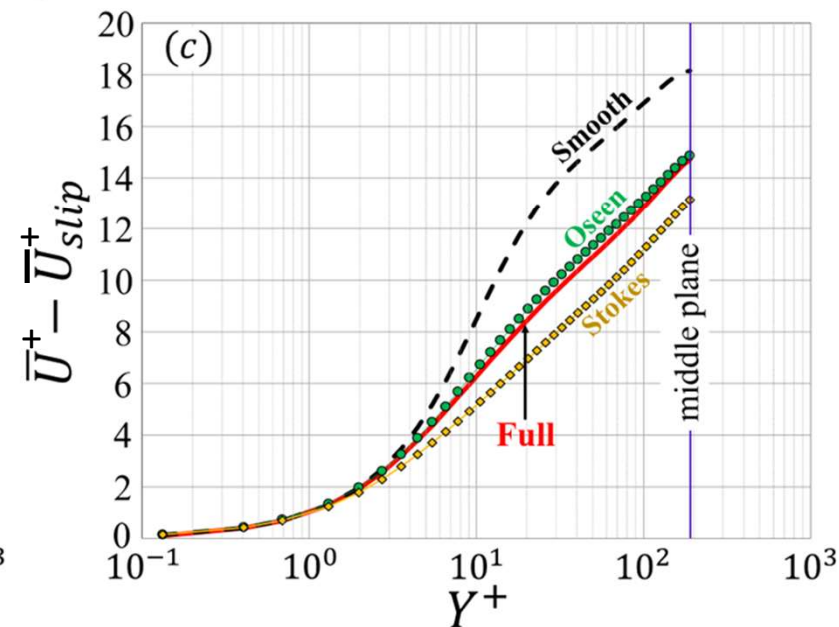
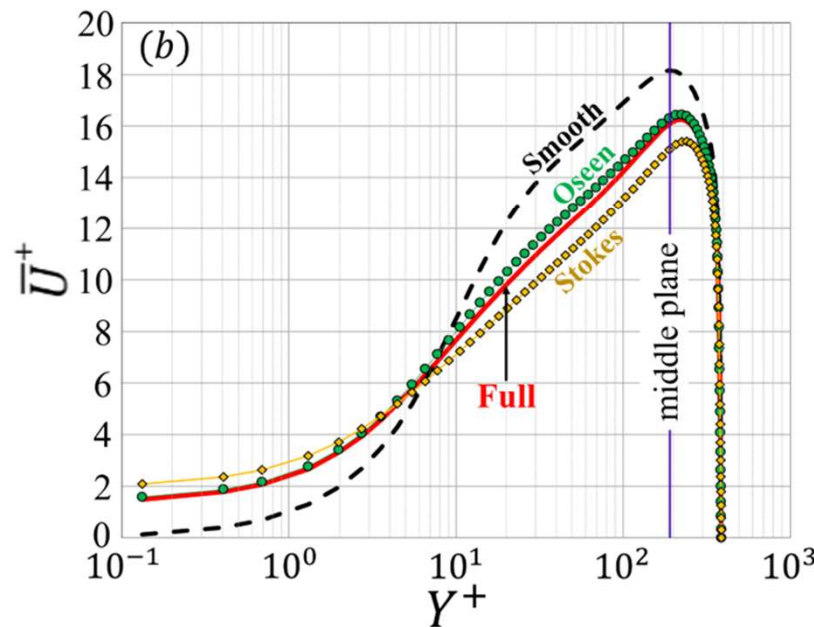
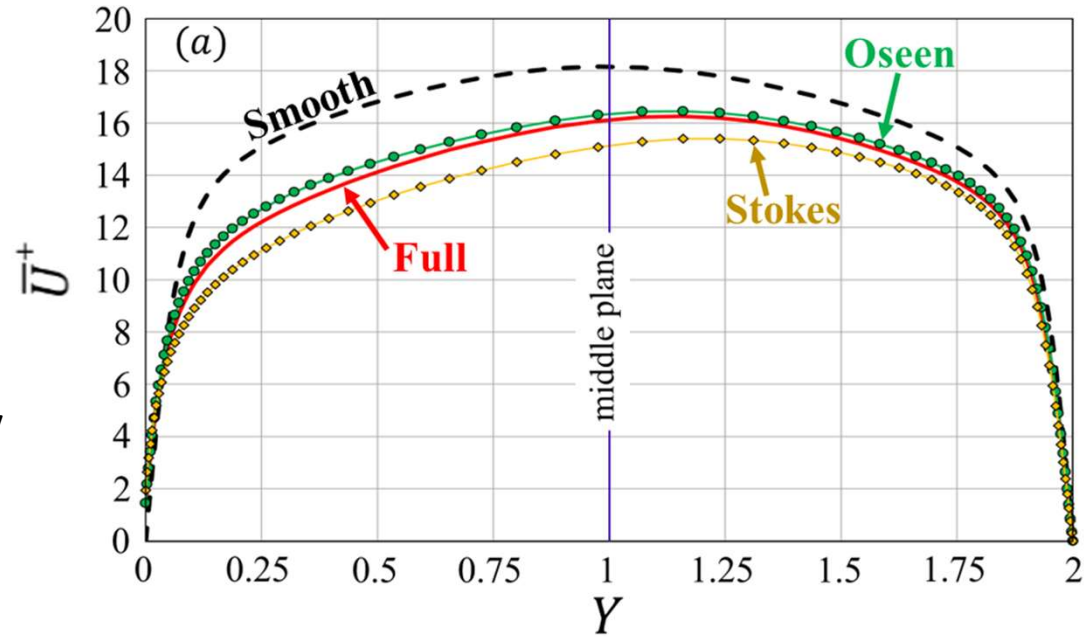


### Model validation

*Transverse cyl.,  $\theta = 0.5$ ,*

$\epsilon = 0.2, Re_\tau \approx 190$

- \* Stokes' model over-estimates drag increase
- \* Oseen's model perfectly predicts slip velocity



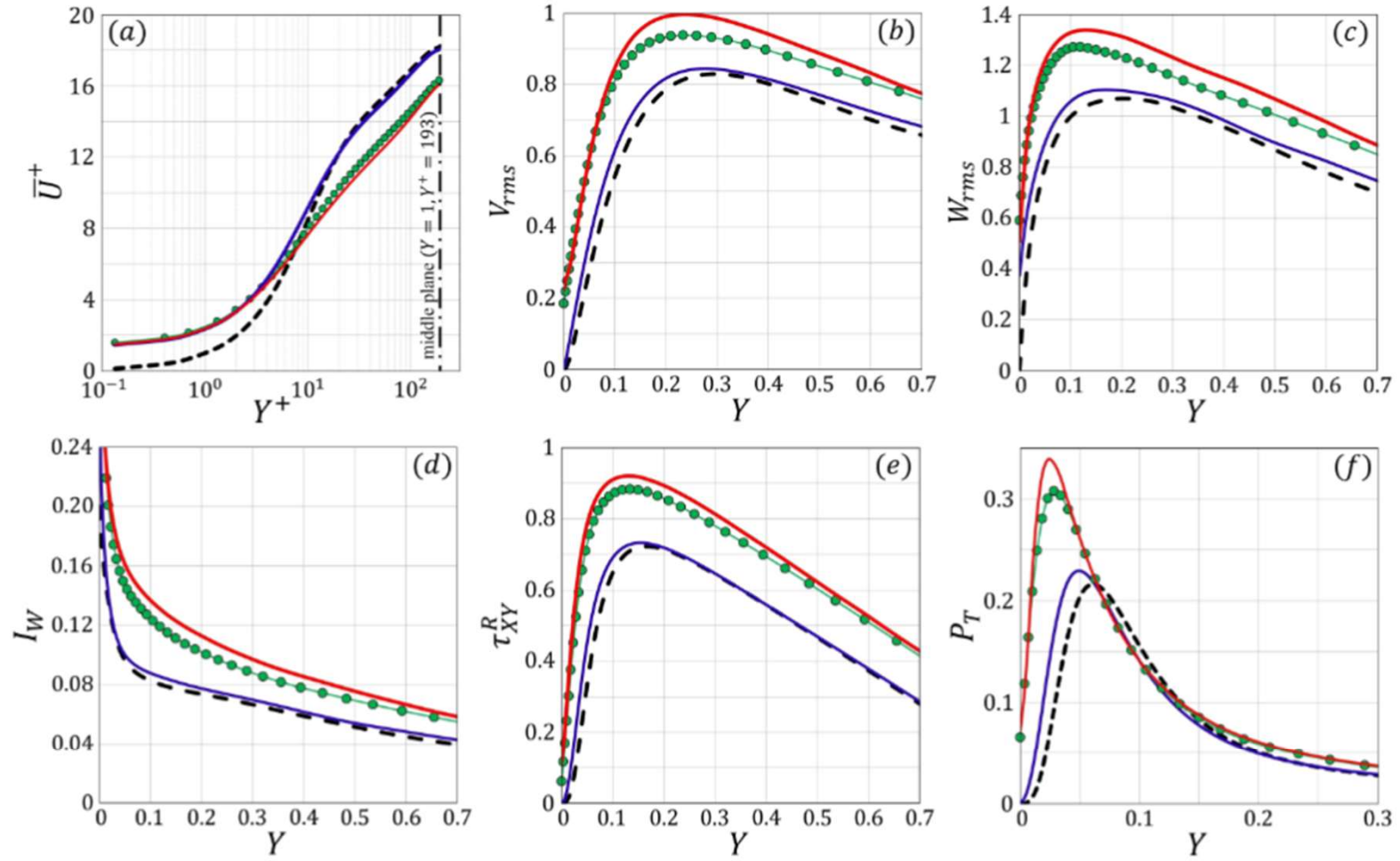
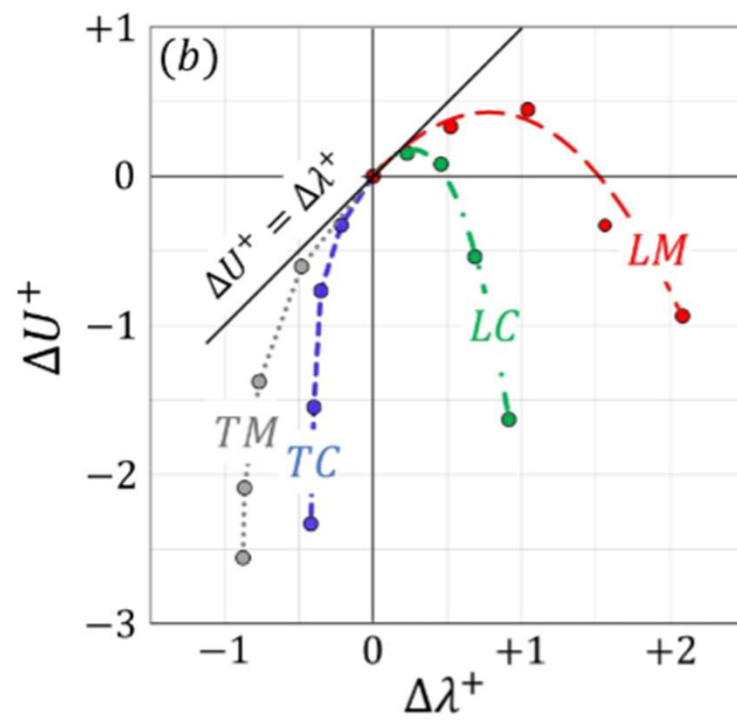
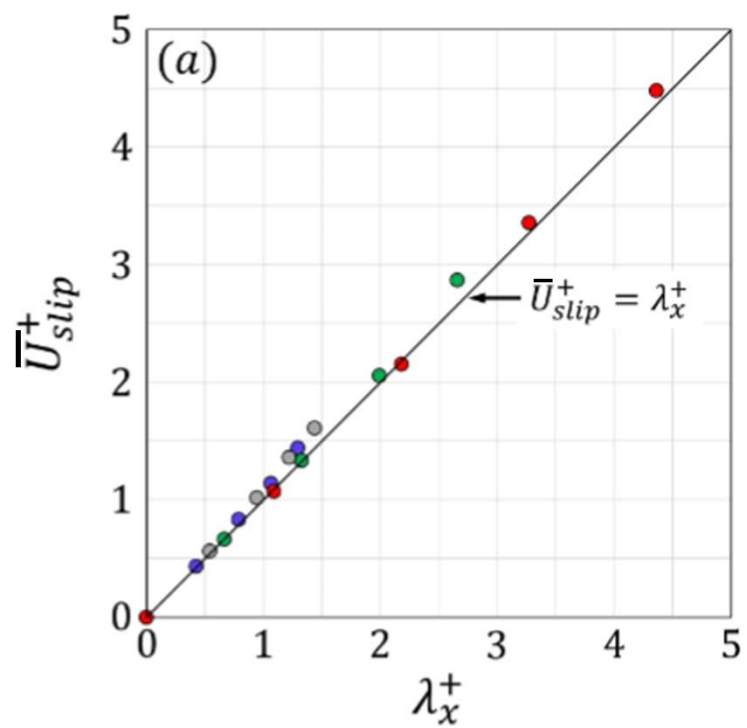
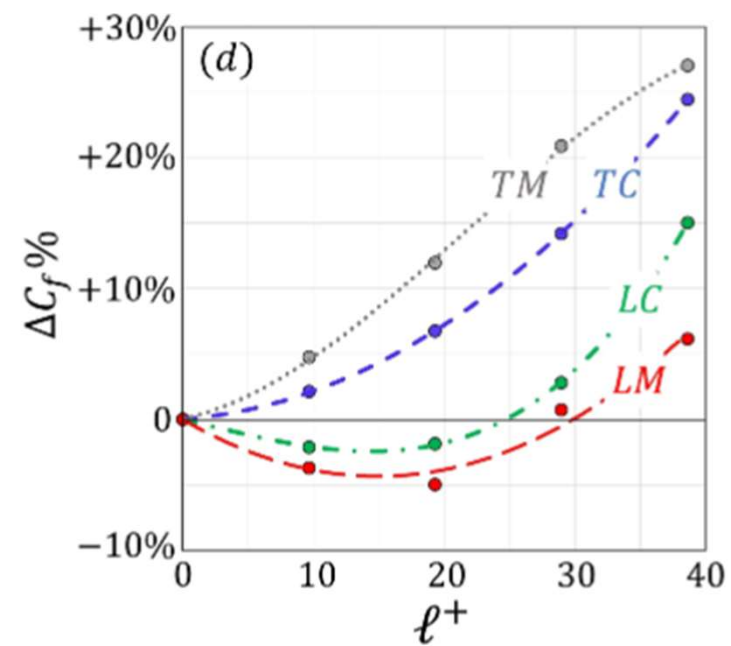
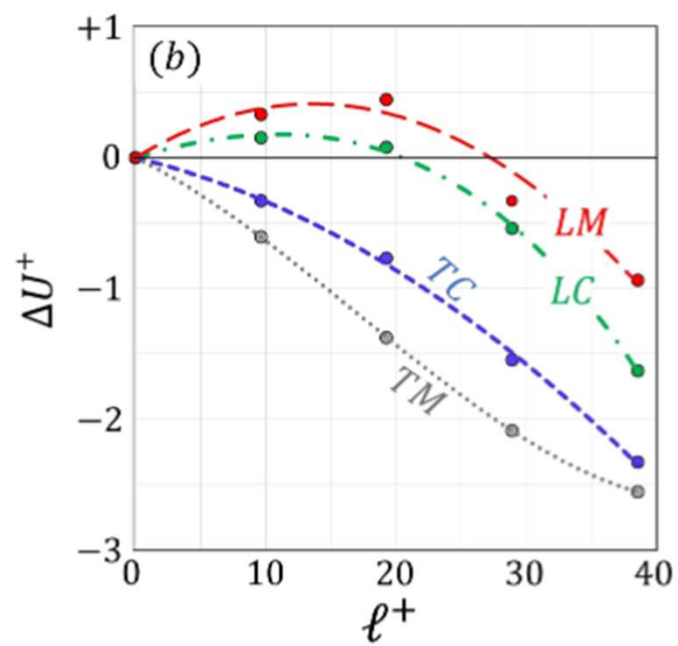
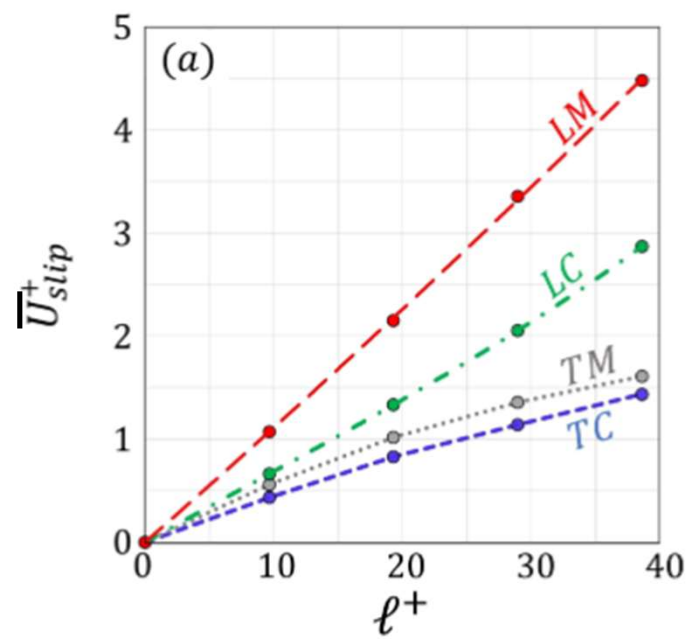
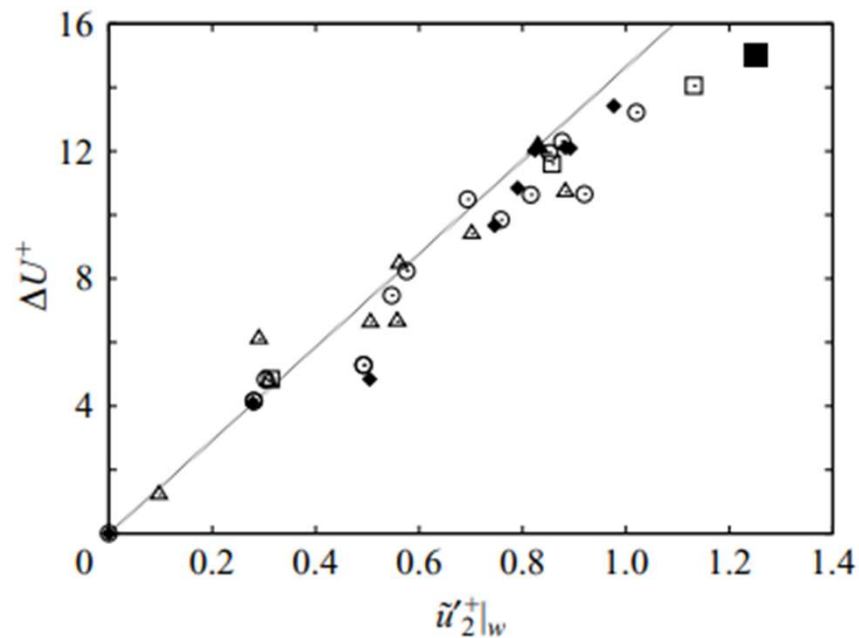


Figure 7: Distribution of the mean velocity (a) and behaviors of quantities of interest related to turbulence statistics (b–f) over the porous substrate  $TC_{20}$ : predictions of the homogenized simulation when the effective boundary conditions of the three velocity components are imposed (green lines with filled circles) or when transpiration is neglected (blue lines) are validated against results of the fine-grained simulation (red lines), while the dashed profiles are related to the smooth, impermeable channel case.



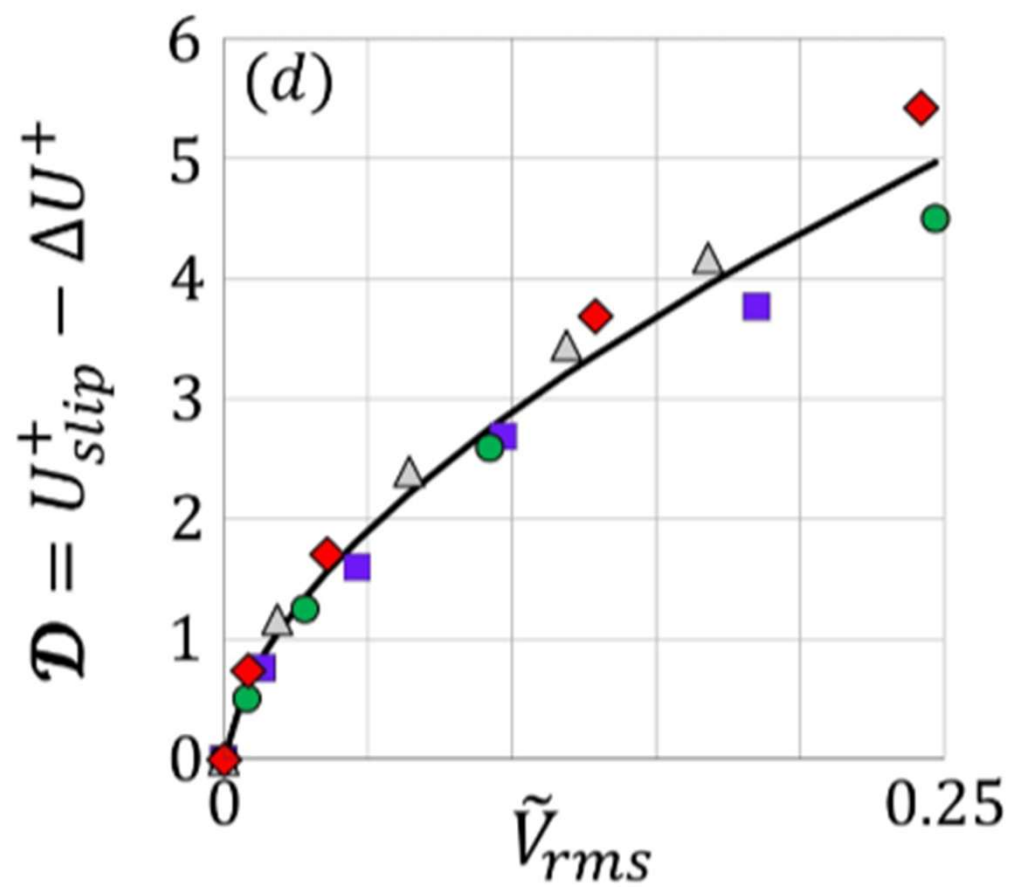


Previous work (Orlandi & Leonardi 2006, 2008) has shown that the roughness function is related to the fluctuating vertical velocity at the fictitious wall



$$\tilde{U}^+ = \kappa^{-1} \ln(\tilde{y}^+) + B \left( 1 - \frac{\tilde{u}'_2{}^+|_w}{\kappa} \right)$$





$$\mathcal{D} = 11.5 \times [\tilde{V}_{rms}]^{0.6}, \quad NRMS_{error} \approx 11\%,$$

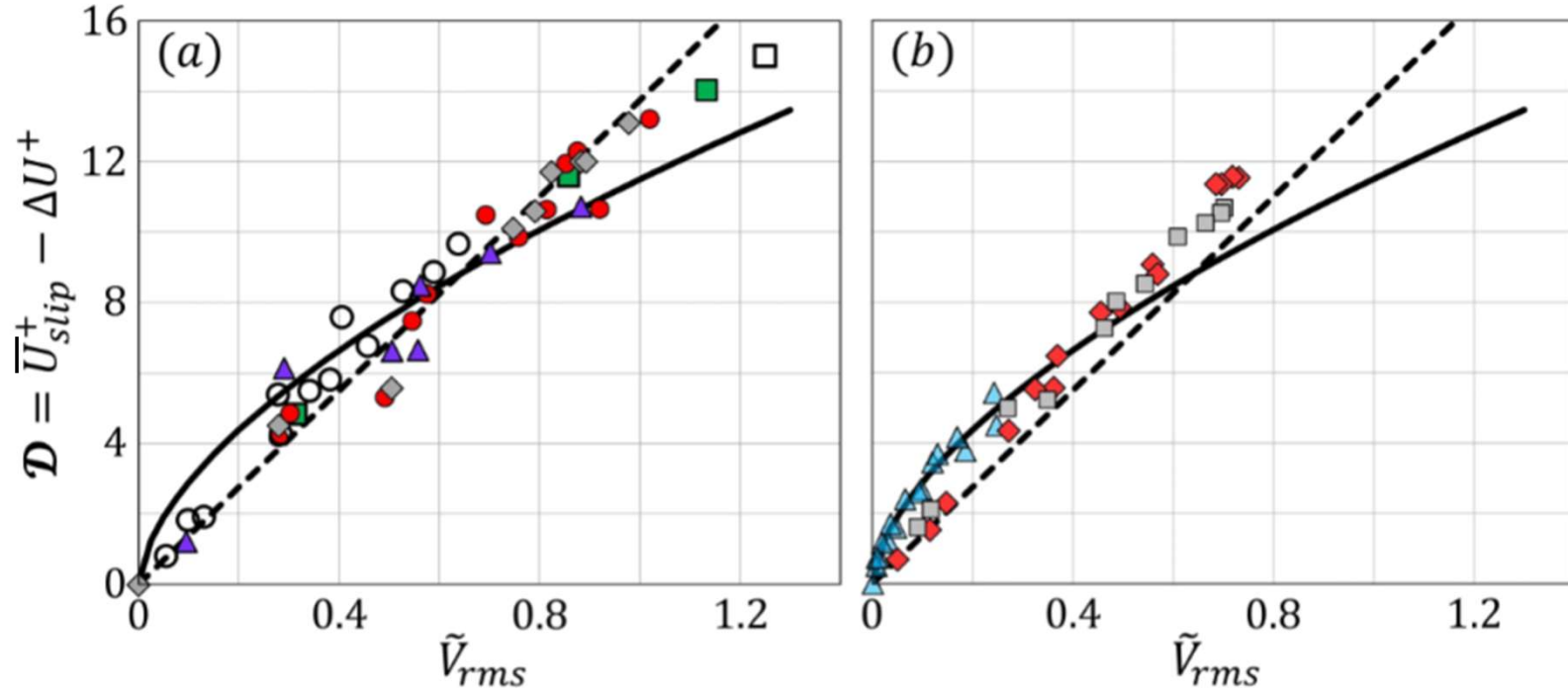


Figure 13: Values of the parameter  $\mathcal{D}$  plotted against the r.m.s. of the turbulent fluctuations in the wall-normal velocity at the plane  $Y = 0$ . In panel (a), results from the literature for channels roughened with streamwise-elongated, spanwise-elongated, or three-dimensional elements are shown: blank square, [Cheng & Castro \(2002\)](#); red circles, [Leonardi \*et al.\* \(2003\)](#); purple triangles, [Orlandi & Leonardi \(2006\)](#); green squares, [Burattini \*et al.\* \(2008\)](#); gray diamonds, [Orlandi & Leonardi \(2008\)](#); blank circles, [Hao & García-Mayoral \(2024\)](#). In panel (b), the results of [Hao & García-Mayoral \(2024\)](#) for symmetric channels bounded by either deep (red diamonds) or shallow (gray squares) porous substrates are plotted, together with the values of the present homogenization-based simulations (light-blue triangles). Solid lines refer to correlation (3.2), while the linear relationship by [Orlandi & Leonardi \(2008\)](#) is plotted with dashed lines.

**But ...**

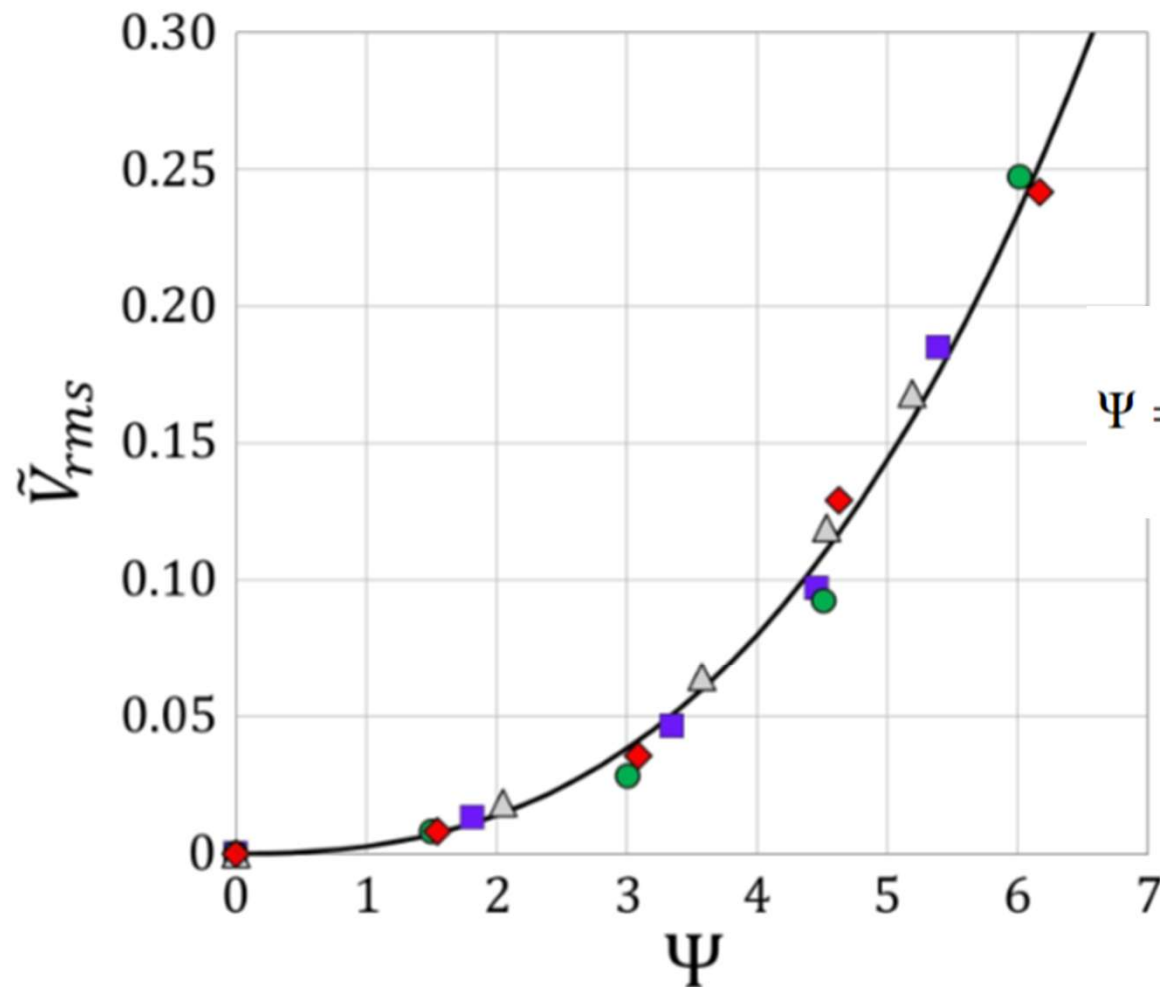
**where do we get  $\tilde{V}_{rms}$  from???**

$$U\Big|_{Y=0^+} = \epsilon \lambda_x \frac{\partial U}{\partial Y}\Big|_{Y=0^+} - \epsilon^2 \operatorname{Re} \mathcal{K}_{xy}^{itf} \frac{\partial P}{\partial X}\Big|_{Y=0^-} + \mathcal{O}(\epsilon^3)$$

$$V\Big|_{Y=0^+} = -\epsilon \frac{\mathcal{K}_{xy}^{itf}}{\lambda_x} \frac{\partial U}{\partial X}\Big|_{Y=0^+} - \epsilon \frac{\mathcal{K}_{zy}^{itf}}{\lambda_z} \frac{\partial W}{\partial Z}\Big|_{Y=0^+} - \epsilon^2 \operatorname{Re} \mathcal{K}_{yy} \frac{\partial P}{\partial Y}\Big|_{Y=0^-} + \mathcal{O}(\epsilon^3)$$

$$W\Big|_{Y=0^+} = \epsilon \lambda_z \frac{\partial W}{\partial Y}\Big|_{Y=0^+} - \epsilon^2 \operatorname{Re} \mathcal{K}_{zy}^{itf} \frac{\partial P}{\partial Z}\Big|_{Y=0^-} + \mathcal{O}(\epsilon^3)$$

Extended Beavers-Joseph-Saffman conditions with NO empirical coefficients

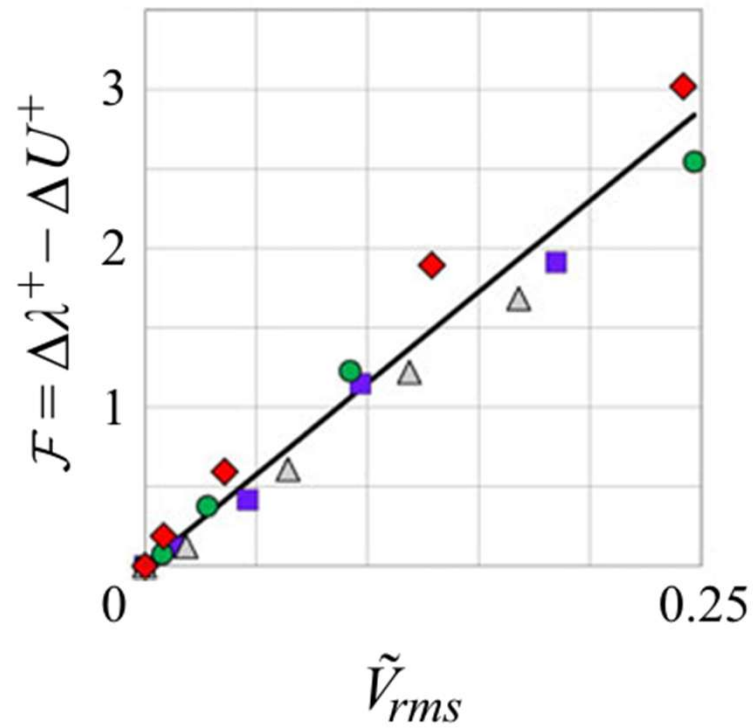


$$\Psi = \left( \frac{\mathcal{K}_{xy}^{itf,+}}{\lambda_x^+} + \frac{\mathcal{K}_{zy}^{itf,+}}{\lambda_z^+} + \sqrt{\mathcal{K}_{yy}^+} \right) \times \left( \frac{\lambda_z^+}{\lambda_x^+} \right)^{0.25}$$

uniquely related to macroscopic  
upscaled coefficients, and easy to  
determine in either the  
approximations of Stokes or Oseen

## Final relation for $\mathcal{D}$

$$\mathcal{D} = \overline{U}_{slip}^+ - \Delta U^+ = 11.5 \times \left( 0.00075 \Psi^3 + 0.002 \Psi^2 \right)^{0.6}$$



$$\mathcal{F} = 11.5 \times \tilde{V}_{rms},$$

$$NRMSE_{error} \approx 18 \%$$

$$\mathcal{F} = \Delta\lambda^+ - \Delta U^+ = 11.5 \times (0.00075 \psi^3 + 0.002 \psi^2)$$

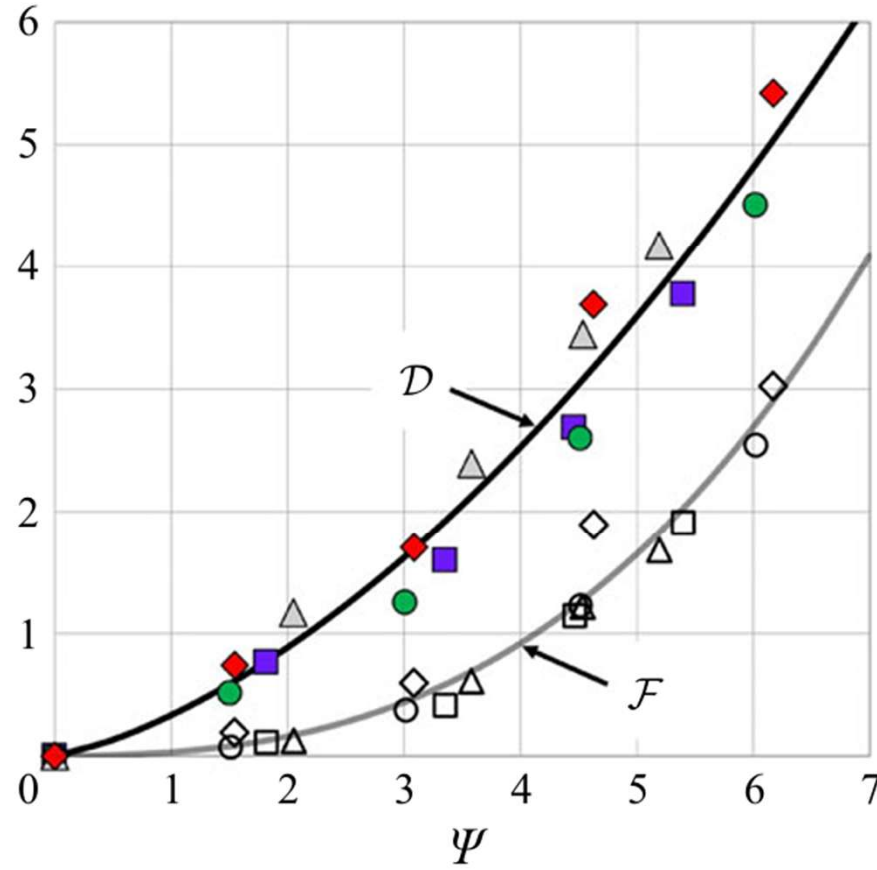


Figure 16. The roughness-function-related quantities  $\mathcal{D}$  and  $\mathcal{F}$ , plotted against the parameter  $\Psi$  for the different porous patterns considered (same symbols as in figure 13, filled for  $\mathcal{D}$  and empty for  $\mathcal{F}$ ). Correlations (3.12) and (3.13) are plotted with solid lines.



**Now we are in the position to make a priori predictions ...**

# Rough wall

$$(\mathcal{K}_{yy} = 0)$$

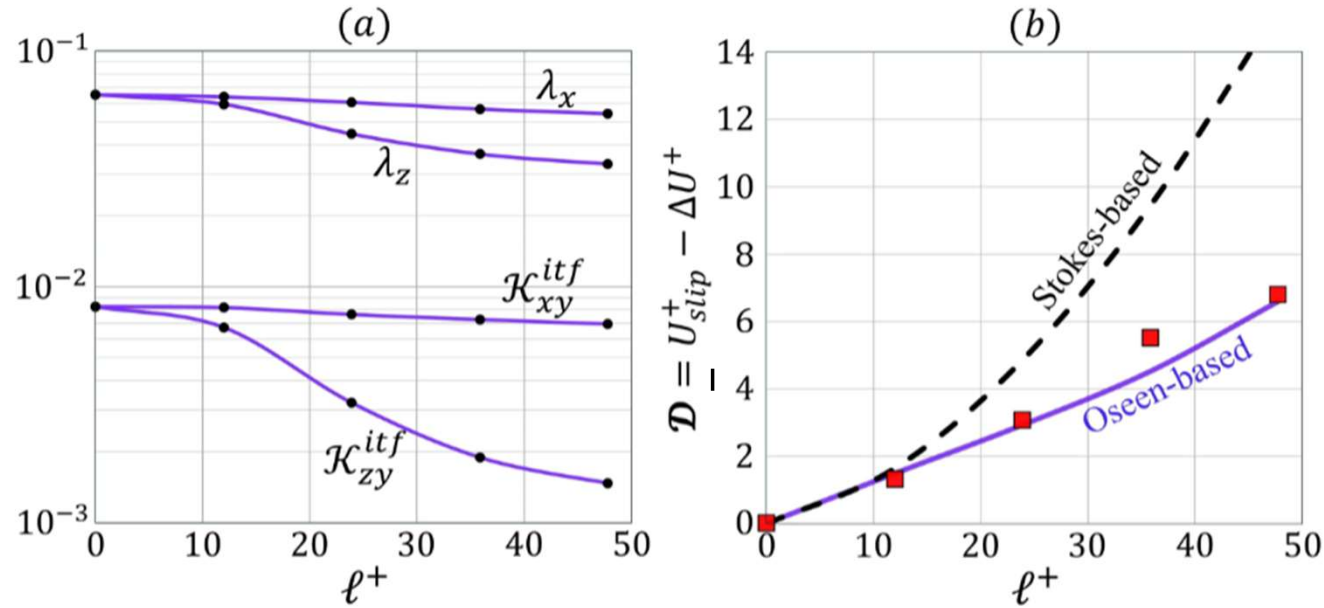


Figure 15: Turbulent flow ( $Re_\tau \approx 180$ ) in a symmetric channel whose top/bottom boundaries are roughened with cubes (in-line arrangement) of size-to-pitch ratio  $e/\ell = 0.5$ , with the spacing in wall units,  $\ell^+ = \epsilon Re_\tau(\mathcal{M})$ , varied up to 50. Values of the macroscopic coefficients are plotted against  $\ell^+$  in panel (a). In panel (b), the behavior of the parameter  $\mathcal{D}$  based on (3.11) is shown (blue curve), and is validated against the results by Hao & García-Mayoral (2024) obtained from full simulations (squares). The black dashed curve refers to the predictions of (3.11) when  $\Psi$  is evaluated with the Stokes-based upscaled coefficients, neglecting near-wall inertia; they are  $\lambda_x = \lambda_z \approx 0.0653$  and  $\mathcal{K}_{xy}^{itf} \approx \mathcal{K}_{zy}^{itf} = 0.0083$ .

# Riblets

$$(\mathcal{K}_{yy} = 0)$$

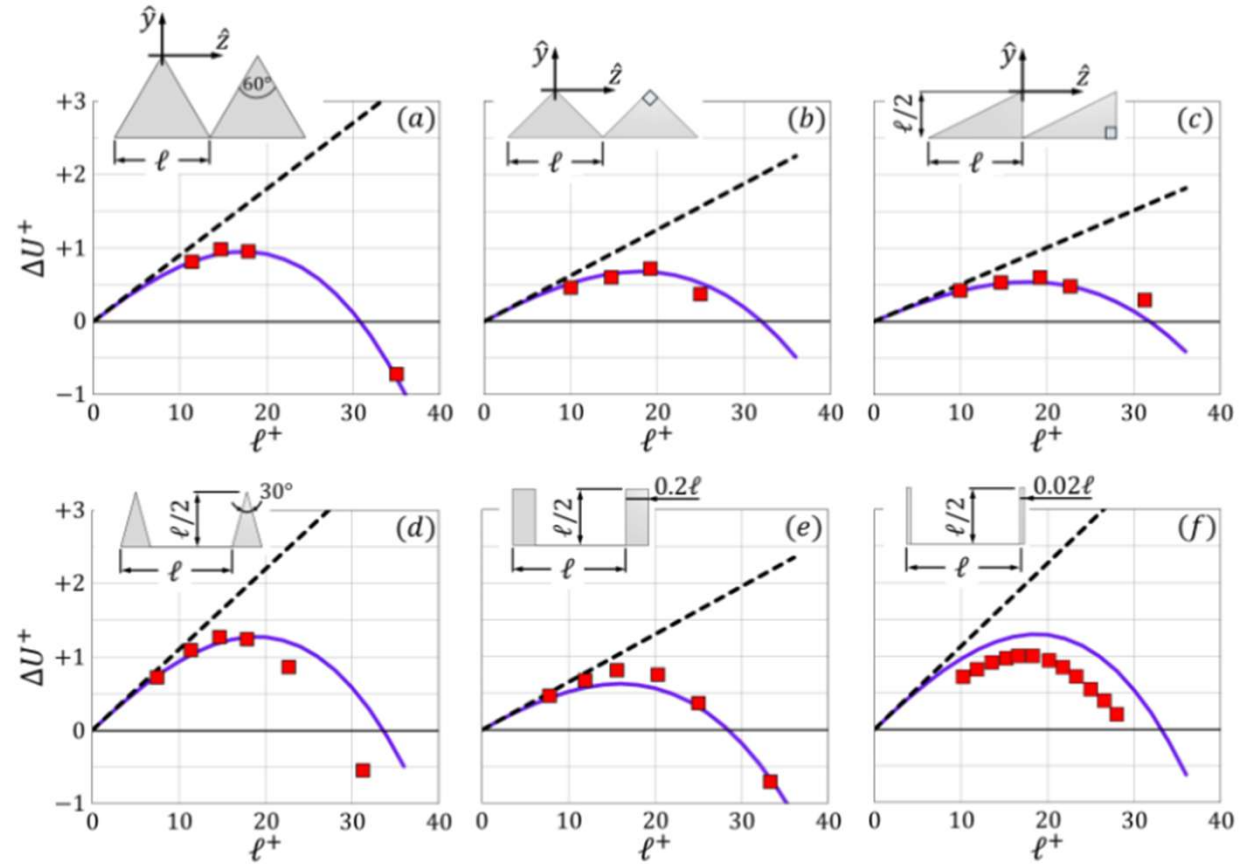
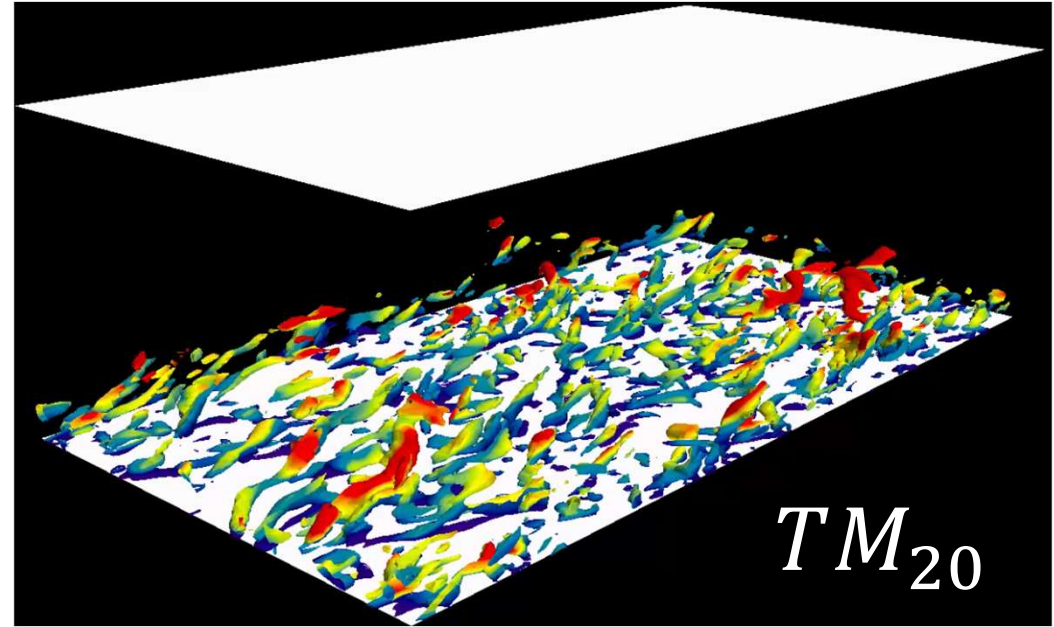
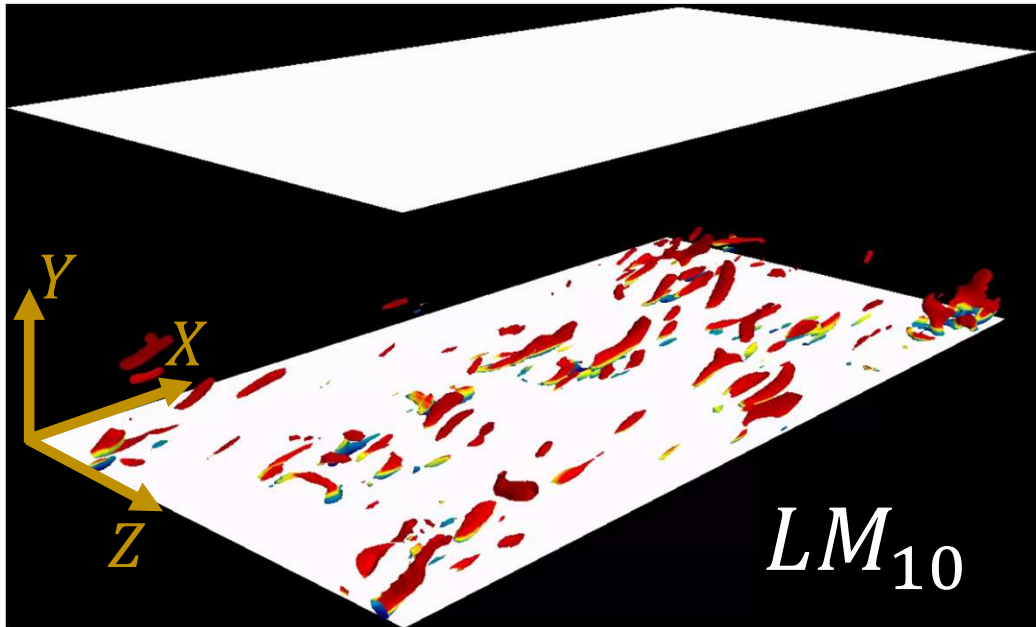


Figure 16: Behavior of  $\Delta U^+$  with the increase in  $\ell^+$ , for the turbulent flow over surfaces with different shapes of riblets. The proposed correlation (blue solid lines) is validated against relevant results from the literature (red symbols), while the black dashed lines represent the simple linear dependence  $\Delta U^+ = \lambda_x^+ - \lambda_z^+$ . The literature results plotted are by (a–e) [Wong \*et al.\* \(2024\)](#) and (f) [Bechert \*et al.\* \(1997\)](#); the latter were reported originally in terms of  $\frac{\Delta C_f}{C_{f,smooth}}$  and the corresponding values of  $\Delta U^+$  are obtained here employing the relation 
$$\Delta U^+ = -\frac{\Delta C_f}{C_{f,smooth}} \times [(2C_{f,smooth})^{-0.5} + 1.25].$$

# Salient ideas

- Homogenization theory can include advection within a linearized (Oseen-like) framework. The theory yields **macroscopic upscaling coefficients**
- Effective wall conditions appear to mimic very well the effect of the surface/substrate
- The drag-reducing/increasing effect of a porous substrate or of wall roughness  $\Delta U^+$  can be reproduced simply by identifying the macroscopic upscaling coefficients, and then computing the **characteristic function**  $\Psi$

Isosurfaces with  $\lambda_2$  *criterion* = 500

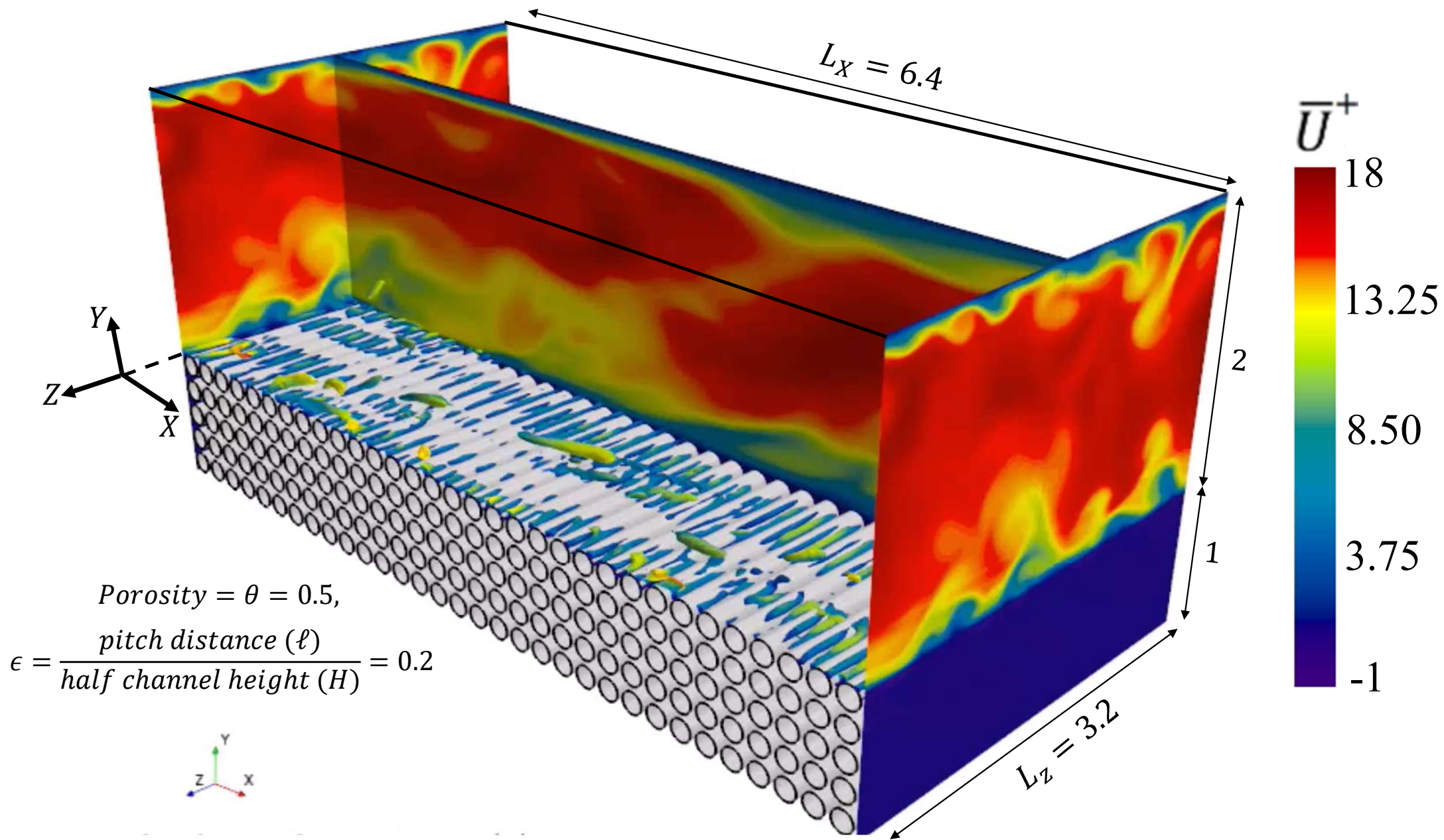


$U$

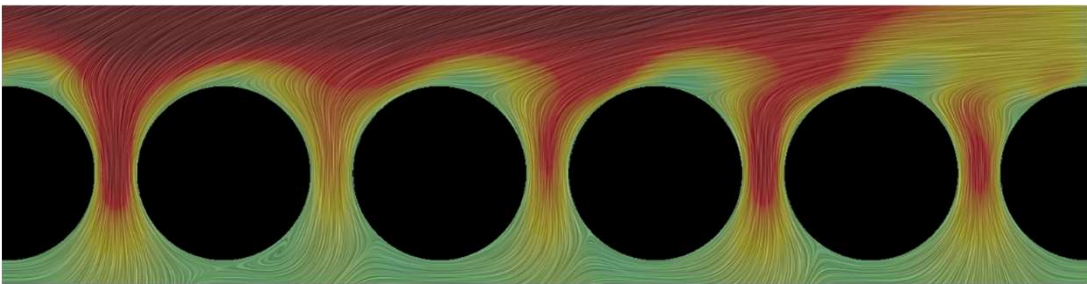


physical time period:  $\Delta T^* = 1$

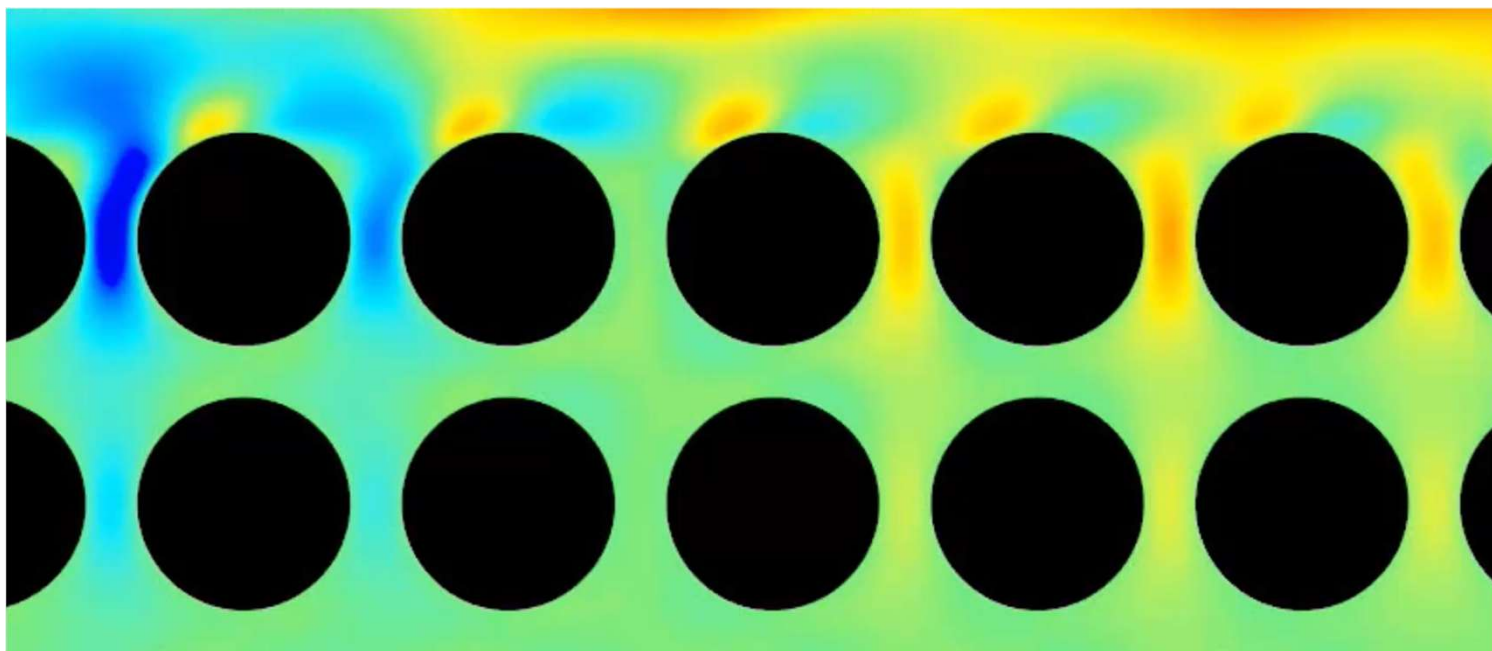
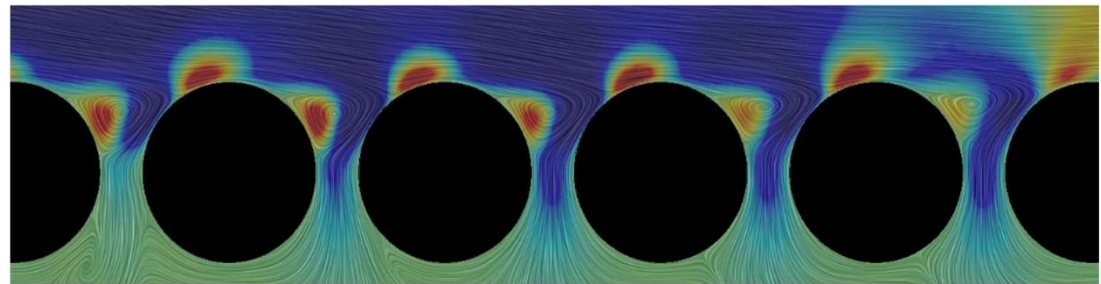




Blowing events



Suction events



physical time period:  $\Delta T^* \approx 5$

